



Cite this: DOI: 10.1039/d5fb00319a

## Valorization of areca nut husk and water hyacinth fibers into biodegradable plates for sustainable packaging

Bedanta Rajbongshi, Akuleti Saikumar\* and Laxmikant S. Badwaik  \*

This study investigates the development of biodegradable plates using cellulose fibers derived from areca nut husk and water hyacinth, aiming to create an eco-friendly alternative to conventional plastic plates and mitigate environmental concerns associated with non-degradable packaging. Raw fibers from both sources were treated with an alkali solution to enhance surface properties. Alkali-treated fibers from both sources were blended in various proportions, doped with starch as a binding agent, and processed *via* thermo-expansion to develop biodegradable plates. Alkali treatment showed significant improvements in the physical properties of both areca nut husk and water hyacinth fibers. Specifically, for areca nut husk, the moisture content dropped from  $13.19 \pm 1.21\%$  to  $9.43 \pm 0.97\%$ , bulk density increased from  $0.137 \pm 0.012$  to  $0.828 \pm 0.030 \text{ g cm}^{-3}$ , and the water absorption index decreased from  $8.59 \pm 0.77$  to  $6.69 \pm 0.32 \text{ g g}^{-1}$ . In parallel, water hyacinth fibers showed a reduction in moisture content from  $14.76 \pm 0.86\%$  to  $10.54 \pm 0.69\%$ , an increase in bulk density from  $0.159 \pm 0.008$  to  $0.413 \pm 0.013 \text{ g cm}^{-3}$ , and a decline in the water absorption index from  $10.34 \pm 0.33$  to  $6.14 \pm 0.41 \text{ g g}^{-1}$ . Among the tested formulations, plates made from a 50 : 50 blend of alkali-treated areca nut husk and water hyacinth fibers exhibited desirable properties like a thickness of  $1.93 \pm 0.06 \text{ mm}$ , grammage of  $1315.67 \pm 20.55 \text{ g m}^{-2}$ , bulk density of  $0.18 \pm 0.02 \text{ g cm}^{-3}$ , moisture content of  $10.27 \pm 0.26\%$ , water absorptiveness of  $481.33 \pm 61.04 \text{ g m}^{-2}$ , and tensile strength of  $3.99 \pm 0.31 \text{ MPa}$ . Furthermore, coating with beeswax significantly improved the water resistance and overall properties of the plate. Biodegradability tests revealed that plates exposed to soil exhibited nearly 70–75% mass loss within 6 weeks. This innovative approach not only offers a practical solution for sustainable packaging but also addresses the environmental challenges posed by agricultural waste and invasive plant species.

Received 27th June 2025  
Accepted 6th October 2025

DOI: 10.1039/d5fb00319a  
[rsc.li/susfoodtech](http://rsc.li/susfoodtech)



### Sustainability spotlight

The development of biodegradable plates using cellulose fibers of areca nut husk and water hyacinth helps create eco-friendly alternatives to conventional plastic plates and mitigate environmental concerns associated with non-degradable packaging. Alkali treatment enhances the overall properties of fibers. Beeswax coating significantly improved the water resistance of plates and it is suitable for dry and low-moisture food packaging. Utilization of agricultural waste and invasive plants for biodegradable plates is a sustainable approach. This innovative approach not only offers a practical solution for sustainable packaging but also addresses the environmental challenges posed by agricultural waste and invasive plant species.

## 1. Introduction

The global packaged food market has achieved remarkable growth in recent years. The ongoing growth of packaged food can be attributed to the convenience, technological progress, and advantages of packaging.<sup>1</sup> However, there is growing concern about the environmental impact of packaging, particularly when considering its effects across the entire lifecycle. The current state of the packaging waste management sector

falls short of achieving circularity because a significant portion of food packaging is intentionally designed for one-time use and subsequently discarded within a brief time frame. Over the past five decades, plastics have been extensively employed in producing packaging materials owing to their effectiveness and ease of manufacturing. Nevertheless, their resistance to natural decomposition has led to significant detrimental impacts on our planet's delicate environment.<sup>2</sup> The food packaging industry is experiencing significant growth within the realm of synthetic plastic packaging.<sup>3</sup> In the pursuit of eco-friendly alternatives to replace traditional plastic packaging, there has been a significant focus on developing biodegradable and biomass-based solutions.

Department of Food Engineering and Technology, School of Engineering, Tezpur University, Napaam, Assam, India. E-mail: [laxmikanthbadwaik@gmail.com](mailto:laxmikanthbadwaik@gmail.com); [saikumarakuleti019@gmail.com](mailto:saikumarakuleti019@gmail.com); Fax: +91-03712-267005; Tel: +91-9706368117

Biodegradable packaging materials, cutlery, and serving items are gaining attention as sustainable alternatives because they naturally break down in the soil through microbial activity, resulting in reduced environmental pollution. Current research in this field focuses on utilizing agro-based polymers and agricultural by-products to create these biodegradable products.<sup>4</sup> While using by-products can help lower raw material expenses, the additional manufacturing processes involved may increase the final price. Despite these challenges, the reuse of agricultural by-products presents a promising avenue, providing both economic and environmental benefits by promoting sustainable packaging production.<sup>5</sup> Bio-based materials, especially natural cellulosic fibers, have gained significant interest due to their rapid decomposition, renewability, and ability to address environmental and health concerns. These fibers are widely used as reinforcements in composites to enhance key properties, such as moisture resistance and tensile strength. Increasingly adopted for their lightweight, biodegradable, carbon-neutral, and renewable nature, natural fibers support the creation of stronger, more durable, and more sustainable packaging solutions.<sup>6-8</sup>

Despite several benefits as reinforcement materials, natural fibers also have drawbacks, such as thermal instability, high moisture absorption, and poor adhesion to hydrophobic polymer matrices, which lead to dimensional instability and reduced mechanical performance.<sup>9-11</sup> The hydrophilic nature of fibers originates from hydroxyl (-OH) groups present in cellulose, hemicellulose, and lignin, which readily form hydrogen bonds with water molecules and prevent effective fiber-matrix interaction. This results in weak interfacial bonding, swelling, and reduced composite durability.<sup>9,12,13</sup> To overcome these limitations, various effective chemical treatments for surface modification of fibers have been employed. Chemical treatments, such as alkalization, bleaching, and acetylation, reduce the number of hydroxyl groups, remove hemicellulose, lignin, and other impurities, and expose purified cellulose, which enhances fiber reactivity and compatibility with the polymer matrix.<sup>14-16</sup> These treatments improve fiber-matrix adhesion, leading to better stress transfer and enhanced composite performance. Studies have shown that alkali treatment with 5-6% NaOH solution significantly improves the mechanical and thermal performance of fiber composites by increasing adhesion and removing hydrophilic components.<sup>9,15,16</sup>

In the present study, alkali-treated cellulose fibers derived from areca nut husk and water hyacinth were used to develop biodegradable plates. Areca nut (also known as betel nut) is cultivated in over 12 Asian nations, yielding approximately 2.28 million tonnes annually from around 1.31 million hectares of farmland (FAOSTAT, 2023) and supporting the livelihoods of more than 10 million farmers.<sup>17,18</sup> India holds a prominent position in the global production of areca nut, occupying the position of the largest producer on a global scale. According to 2017 statistics from the Food and Agriculture Organization (FAO), United Nations, India's output constituted a remarkable 54.07% of the world's total production. However, a substantial issue arises with the byproduct of areca nut processing.<sup>19</sup> After kernels are extracted in small-scale facilities, the generated husk

(dry or green forms) is often discarded in open areas. In India alone, according to the National Horticulture Board (NHB), the production of areca nut fruit in 2021-22 was recorded at 1 371 940 tonnes, and since the fruit contains around 40% husk, an estimated 548 776 tonnes of husk are generated annually. The primary constituents of areca nut husk include cellulose (35-64.8%), with notable amounts of hemicellulose, lignin (13-26%), and approximately 7% of pectin.<sup>20,21</sup> These husks do not readily decompose due to their lignocellulosic composition, leading to environmental challenges as a large pile of husks accumulates due to inadequate disposal methods.<sup>22</sup>

Water hyacinth stands out as one of the most pervasive aquatic weeds globally, known for its rapid growth rate of up to 220 kg per ha per day.<sup>23-25</sup> It can double its population within 5-15 days, depending on site conditions.<sup>26</sup> What makes it particularly troublesome is its exceptional ability to efficiently extract nutrients from water and its high reproductive capacity.<sup>27</sup> Agricultural nutrient runoff and excessive fertilization contribute significantly to its massive proliferation, causing the swift degradation of aquatic ecosystems.<sup>28</sup> The robust expansion of water hyacinth mats has detrimental effects of reducing dissolved oxygen levels and evapotranspiration, which causes increased water loss.<sup>29,30</sup> Moreover, water hyacinth tends to clog irrigation canals and cause rapid silt accumulation, resulting in inefficient flood control measures and lowering water quality for productive water uses.<sup>31</sup> Due to these issues, numerous management strategies for tackling this weed have been implemented, involving expensive methods like chemical, physical, or biological controls. However, most of the existing approaches have provided short-term reductions in biomass and are cost-intensive and unsustainable.<sup>32</sup> For example, heavy machinery can remove infestations rapidly, but the weeds can regrow within a few weeks in stagnant, nutrient-rich water. Chemical herbicides may show impact in days but can harm non-target aquatic species and pose ecological risks.<sup>33,34</sup> Due to these challenges, there is a growing need for more sustainable solutions, such as converting this plant biomass into biodegradable materials through fiber-based valorization. Water hyacinth is a non-wood lignocellulosic material comprising cellulose (65.07%), hemicellulose (15.17%), and lignin (11.38%) as reported by Sumrith *et al.*<sup>35</sup> Its higher cellulose and hemicellulose content, along with lower lignin compared to both woody and non-woody plants, make it ideal for pulp production. This pulp can be utilized in diverse packaging applications due to these unique composition characteristics.<sup>36</sup>

There has been a remarkable absence of research regarding the prospect of producing biodegradable plates from cellulose fibers derived from areca nut husk and limited exploration of the applicability of water hyacinth in this context. This research work seeks to address two environmental challenges, the management of areca nut husk waste and the proliferation of aquatic weed water hyacinth, by pioneering the development of biodegradable food plates from these sustainable sources. This work investigates the synergistic use of areca nut husk and water hyacinth, a combination that has not been previously explored for biodegradable plate fabrication. Blending different biomass fibers has been reported to improve composite properties by combining the



strength of rigid fibers with the flexibility or network-forming ability of softer ones (*e.g.*, paddy straw with pine needles; sugarcane bagasse with bamboo).<sup>37,38</sup> Therefore, the proposed research aims to utilize alkali-treated fibers derived from areca nut husk and water hyacinth in conjunction with natural starch-based polymers to develop biodegradable plates with beeswax coating to enhance mechanical strength and water barrier properties. This integrated dual-fiber and surface-modification approach evaluates the structural, functional, and biodegradability characteristics of the plates for sustainable food packaging or serving applications.

## 2. Materials and methods

### 2.1. Collection of raw materials

Husks of matured areca nuts were procured from local households in Napaam, Tezpur ( $26.6528^{\circ}$  N,  $92.7926^{\circ}$  E), Assam, India. Water hyacinth plants with stalks and leaves were collected from the waterbodies near the Tezpur University campus, Tezpur, Assam, India. Commercial food grade tapioca starch was supplied by Kritavin Pvt. Ltd (New Delhi, India), beeswax (solubility:  $33.3\text{ mg mL}^{-1}$  of chloroform, melting range:  $61\text{--}65^{\circ}\text{C}$ , acid value: 5–15, ester value: 75–95, and saponification value: 87–104) and guar gum (presence of starch, acid insoluble matter  $\leq 7\%$ , sulphated ash  $\leq 1.5\%$ , protein  $\leq 10\%$ , and galactomannans  $\leq 70\%$ ) were supplied by Hi-Media Laboratories Private Ltd (Mumbai, India), glycerol was procured from Merck Life Science Pvt. Ltd (New Delhi, India), and sodium hydroxide was procured from Finar Chemical Limited, Ahmedabad (India).

### 2.2. Preparation of areca nut husk and water hyacinth fibers

After removing the roots, the stalk and leaves of the water hyacinth were separated and cut into small pieces and washed under tap water. The raw areca nut husk and water hyacinth were then dried for 12 h at  $70^{\circ}\text{C}$  and subsequently soaked separately in 6% NaOH solution at room temperature ( $25\text{--}30^{\circ}\text{C}$ ) for 24 h and 12 h, respectively. The concentration of alkali solution and soaking duration of fibers were chosen based on the preliminary trials and protocols reported in the literature for treating natural fibers.<sup>39–42</sup> After discarding the NaOH solution, fibers were immersed in distilled water for 2 h to remove the residual NaOH and soaked again in distilled water containing a small amount of 2% acetic acid. Finally, the fibers

further use. Alkali-treated fibers were dried in an oven at  $70^{\circ}\text{C}$  for 24 h.<sup>39</sup> The alkali-treated fibers were pulverized and sieved through a mesh with a size of BSS (410/1969)-52 for uniformity (300 microns). The processed fibers were then carefully stored in distinct PVC airtight containers to maintain their integrity and prevent environmental contamination.<sup>43</sup>

### 2.3. Characterization of fibers

To check the effectiveness of the alkali treatment, the raw and alkali-treated areca nut husk and water hyacinth fibers were analysed for their various properties, including physical properties, functional properties, FTIR, and thermal properties.

**2.3.1. Physical properties of fibers.** The moisture content (MC) of the fiber was determined using the hot air oven method, where a measured weight of the fiber was placed in a hot air oven at  $105 \pm 2^{\circ}\text{C}$  for 4 h or until a constant weight was observed.<sup>44</sup> Bulk density (BD) was measured by placing 2 g of fiber into a 10 mL measuring cylinder, followed by vortex vibration for 1 minute.<sup>45</sup> True density (TD) was determined by placing 2 g of fiber in a 25 mL density bottle using distilled water as the displacement fluid, and the final volume was used to calculate TD.<sup>46</sup> Porosity was calculated by subtracting the ratio of BD and TD from one.

**2.3.2. Functional properties of fibers.** The water absorption index (WAI) and oil absorption index (OAI) were determined by mixing 1 g of fiber with 20 mL of distilled water for the WAI and edible oil for the OAI in centrifuge tubes. The mixtures were allowed to stand at  $30 \pm 2^{\circ}\text{C}$  for 30 min, agitated for 2 min, and then centrifuged at 4000 rpm for 20 min. After centrifugation, the supernatant was decanted, and the residue-containing tubes were reweighed to calculate the WAI and OAI using eqn (1).<sup>47,48</sup> Similarly, water swelling power (WSP) and oil swelling power (OSP) were measured by mixing 1 g of fiber with 20 mL of distilled water or edible oil in a conical flask and heating the mixture at  $90^{\circ}\text{C}$  in a water bath with continuous stirring for 30 min, followed by cooling and transferring it to pre-weighed centrifuge tubes. These were centrifuged at 5000 rpm for 20 min at room temperature, and the wet sediment was weighed to calculate WSP and OSP using eqn (2).<sup>49</sup>

$$\text{WAI/OAI}(\text{g g}^{-1}) = \frac{\text{weight of residual after centrifugation}(\text{g})}{\text{initial dry weight of fiber}(\text{g})} \quad (1)$$

$$\text{WSP/OSP}(\text{g g}^{-1}) = \frac{\text{weight of swollen sediment after heating and centrifugation}(\text{g})}{\text{initial dry weight of fiber}(\text{g})} \quad (2)$$

were washed repeatedly 2–3 times to remove the last traces of acid. The pH of each fiber batch was measured and found to be around neutral ( $7 \pm 0.2$ ). If the pH was not neutral, additional washing was carried out to remove any remaining acidic residues, ensuring that the fibers were properly cleaned and safe for

**2.3.3. FTIR analysis of fibers.** Fourier Transform Infrared Spectroscopy (FTIR, Frontier MIR, PerkinElmer, USA) was used from  $400\text{--}4000\text{ cm}^{-1}$  with a resolution of  $4\text{ cm}^{-1}$  to determine the chemical structure of fibers. FTIR spectra of the raw and alkali-treated fibers were recorded using the attenuated total



reflection (ATR) technique. Using Origin software, peak heights were determined from the absorbance spectra.<sup>35</sup>

**2.3.4. Thermal analysis of fibers.** Differential scanning calorimetry (DSC) (DSC 214 Polyma, NETZSCH, Germany) was used to investigate the thermal characteristics. Samples of raw and alkali-treated areca nut husk and water hyacinth fibers were positioned on an aluminium pan within a nitrogen atmosphere. The analysis was carried out from room temperature to a maximum temperature of 400 °C at a heating rate of 10 °C min<sup>-1</sup> under a nitrogen flow of 50 mL min<sup>-1</sup>. The fiber's phase properties were depicted through a DSC thermogram.<sup>44</sup>

#### 2.4. Preparation of biodegradable plates

For the development of the plate, a dough was formulated to provide the structural matrix of the plate. This formulation includes tapioca starch serving as the binding agent, guar gum to prevent starch settling, and glycerol as a plasticizer to provide flexibility to the plate. The addition of guar gum improves matrix uniformity and enhances the homogeneity and moldability of the dough, whereas glycerol reduces intermolecular forces between polymer chains, improves flexibility, and reduces cracking during molding and drying of the plates.<sup>50-57</sup> In the first step, a solution was prepared by adding 5 g of tapioca starch, 3 g of guar gum, and 3 mL of glycerol as a plasticizer in 100 mL of distilled water. The resulting solution was homogenized at 1000 rpm for 5 min and subsequently heated to the gelatinization temperature (~ 65 °C) of the starch.<sup>58,59</sup> A dough was prepared by adding 20 g of dried fibers in different ratios into the above solution and used for making plates (Table 1). The total amount of fiber was maintained constant at 20 g across all the formulations.

The dough was heat-pressed manually, and the process was carried out in a circular-shaped double heat pan press mold (Mazoria, TCB-1, baking machine, India). It is powered by 230 V AC and is equipped with temperature control. Before being subjected to heat pressing, the mold was preheated to 150 °C for 2 min to ensure uniform heating. The prepared dough was placed on the bottom pan and pressed down manually with the upper pan for 7 ± 2 min at 110 °C. The prepared plates were stored for one week in a controlled environmental chamber at 50% RH and 25 °C. This step ensures moisture equilibration and structural stabilization before testing physical and mechanical properties.

Table 1 Proportions of fibers for the biodegradable plate

Plate composition number	Areca nut husk fiber (%)	Water hyacinth fiber (%)
C <sub>1</sub>	100	0
C <sub>2</sub>	80	20
C <sub>3</sub>	60	40
C <sub>4</sub>	50	50
C <sub>5</sub>	40	60
C <sub>6</sub>	20	80
C <sub>7</sub>	0	100

#### 2.5. Hydrophobic coating of biodegradable plates

The developed plates were selected for the coating to enhance their water barrier properties and thereby facilitate their application in food packaging or serving purposes. Beeswax was chosen due to its natural abundance, safety for food contact, and demonstrated effectiveness in previous studies and was preferred over other biopolymers such as shellac or chitosan due to its lower cost, easier processing, and higher moisture-barrier properties.<sup>43,60,61</sup> Beeswax, after being liquefied, was applied onto the plate surfaces. This was achieved by melting the beeswax in a beaker within a hot water bath set at 70 °C. The waterproof coating was applied using a dipping method, ensuring a one-layer coating to enhance its barrier capability.<sup>62</sup> After immersion in the molten beeswax, the plates were held vertically to allow excess wax to drip off before cooling, ensuring a uniform coating.

#### 2.6. Properties of the biodegradable plate

**2.6.1. Thickness and grammage.** The thickness of the plate samples was measured using a Vernier calliper. Measurements were conducted at five different positions on the plate, and the average thickness was calculated. The plate's grammage was determined following ISO 536 guidelines.<sup>63</sup> Plate samples measuring 0.01 m<sup>2</sup> were weighed, and the grammage was expressed in g m<sup>-2</sup>.<sup>64</sup>

**2.6.2. Bulk density.** The bulk density (BD) of the plates was measured using the sand displacement method as described by Kaisangsri *et al.*<sup>65</sup> A sample of 20 × 20 mm was weighed and placed in a 50 mL measuring cylinder, followed by the addition of sand. After tapping the graduated cylinder for 1 min, the total volume was recorded, and BD was calculated by dividing mass (g) by the plate volume (mL).

**2.6.3. Moisture content.** The moisture content (MC) of the plate was determined according to ASTM D 644-99 (2002) standards.<sup>66</sup> Plate samples of 20 × 20 mm were taken from three distinct pieces of the plates and stored at a RH of 75% for 24 h at 25 °C. The samples were dried in a hot air oven at 105 °C for 4 h, or until no change in weight was observed in subsequent readings. The percentage of MC in the plates was then calculated based on the weight loss percentage.<sup>65</sup>

**2.6.4. Water absorptiveness.** To evaluate the water absorptiveness of the plates, the Cobb method was used following ISO 535 guidelines.<sup>67</sup> Initially, the samples were weighed and then gradually immersed in 100 mL of water within a cylinder, leaving a 10 mm headspace, with the timer starting immediately for 60 s. After removal from the water, the samples were blotted with absorbent paper to eliminate excess water and weighed again. The absorption capacity of the paper was calculated using eqn (3).

$$\text{Water absorptiveness (g m}^{-2}\text{)} = (m_2 - m_1) \times F \quad (3)$$

where  $m_2$  represents the wet mass of the sample in grams,  $m_1$  represents the dry mass of the sample in grams, and  $F$  is calculated as 10 000 per test area, with a typical apparatus having a test area of 100 cm<sup>2</sup>.<sup>64</sup>



**2.6.5. Absorbency.** The absorbency test evaluates the rate at which a material absorbs liquid using gravimetric principles. To measure absorbency, the plate sample was positioned atop an empty and dry beaker without central support. Using a micro-pipette, precisely 10  $\mu\text{L}$  of water was dropped onto the plate's surface. A stopwatch was started immediately upon releasing the water and stopped once the droplet had completely dispersed through the material.<sup>64</sup>

**2.6.6. Water solubility.** To determine the water solubility, plate samples (4 cm  $\times$  4 cm) were conditioned at  $\sim$ 66% RH for 7 days, weighed, and immersed in 100 mL distilled water with agitation for 1 h. After blotting, samples were dried at 50 °C for 6 h and reweighed. The solubility was then calculated using eqn (4).

$$\text{Water solubility}(\%) = \left( \frac{W_1 - W_2}{W_1} \times 100 \right) \quad (4)$$

where  $W_1$  and  $W_2$  represent the sample weight before and after immersion, respectively.<sup>43,68</sup>

**2.6.7. Measurement of color.** The  $L^*$ ,  $a^*$ , and  $b^*$  color values were measured three times for each biodegradable plate sample using a Hunter Lab colorimeter (Hunter Lab, Reston, Virginia, USA). The overall color variation ( $\Delta E$ ) and the whiteness index were calculated using eqn (5) and (6).<sup>5,69</sup>

$$\Delta E = \sqrt{(L^* - L'^*)^2 + (a^* - a'^*)^2 + (b^* - b'^*)^2} \quad (5)$$

$$\text{Whiteness index} = 100 - \sqrt{(100 - L^*)^2 + a^{*2} + b^{*2}} \quad (6)$$

where  $L'^*$ ,  $a'^*$ , and  $b'^*$  are the mean color values of the plate with 100% areca nut husk fiber ( $C_1$ ).

**2.6.8. Mechanical properties.** The tensile strength (TS) of the plate samples was assessed according to ASTM D3039/D3039M with some modifications using a texture analyzer (Stable Micro System, UK; Model: TA-XD Plus) equipped with a 30 kg load cell.<sup>70</sup> Samples of rectangular size 60  $\times$  20 mm were taken from three distinct portions of the plate. This sampling approach ( $n = 3$ ) was chosen to consider spatial heterogeneity introduced during molding and beeswax coating (e.g., thickness gradients, fiber orientation, etc.). The grip separation was initially set to 20 mm, with a crosshead speed fixed at 2 mm s<sup>-1</sup>. The TA was calculated using eqn (7).

$$\text{Tensile strength (MPa)} = F/A \quad (7)$$

where  $F$  represents the maximum tensile force before rupture and  $A$  is the cross-sectional area of the sample.<sup>65</sup>

**2.6.9. Morphological analysis.** The surface morphology of plates containing areca nut husk and water hyacinth fibers was examined using Scanning Electron Microscopy (SEM) (JEOL JSM-6390 LV; Japan), operating at an applied acceleration voltage of 12 kV. The plate samples were dried at 40 °C for 24 h, then fractured or cut into 3 mm fragments and affixed to aluminium stubs with carbon double-sided tape. These fragments were coated with a thin layer of platinum before SEM analysis to enhance visualization.<sup>71</sup>

## 2.7. Biodegradability test

The test for the biodegradability of the plate samples was carried out by an adapted qualitative test based on the methodology proposed by Engel *et al.*<sup>71</sup> A laboratory-scale soil burial experiment was performed to study the biodegradability of the samples. Vegetable compost (soil) and sand were separately placed in containers, and plate samples (2.5  $\times$  2.5 cm) were buried completely at a depth of 10 cm. Soil was used to simulate natural composting, while sand served as an inert control with lower microbial content. The containers were kept under aerobic conditions at room temperature, with water sprayed daily to maintain soil moisture throughout the experiment. The plate samples were retrieved every 7 days, photographed, and monitored for degradation by measuring the reduction in weight of the samples. The weight loss (% degradation) of the plate samples was calculated using eqn (8).<sup>72</sup>

$$\% \text{ degradation} = \frac{W_i - W_f}{W_i} \times 100 \quad (8)$$

where  $W_i$  is the sample's initial weight (day 0) and  $W_f$  is its weight after removal from the soil (or sand).

## 2.8. Statistical analysis

All the experiments were carried out with three replications, and the obtained data were reported as mean  $\pm$  standard deviation (SD). One-way ANOVA was applied to determine the critical difference of mean and variance among the samples. The Duncan test with equal variances was carried out with a  $P < 0.05$  significance level by using IBM SPSS version 23 software.<sup>73</sup>

## 3. Results and discussion

### 3.1. Physical properties of fibers

The physical properties of raw and alkali-treated areca nut husk and water hyacinth fibers were evaluated to assess their suitability for developing biodegradable plates, and the data are presented in Table 2. The MC, BD, TD, and porosity values were significantly different ( $p < 0.05$ ) for the raw and alkali-treated fibers from both sources. The alkali treatment removes the hydrophilic non-cellulosic components like hemicellulose, lignin, and pectins from the fiber surface, making it more hydrophobic and reducing the MC.<sup>74</sup> The lower MC improves the compatibility of areca nut husk and water hyacinth fibers with polymer matrices in composites. The BD values for raw areca fibers and water hyacinth fibers were  $0.137 \pm 0.012$  and  $0.159 \pm 0.008 \text{ g cm}^{-3}$ , respectively, which increased to  $0.828 \pm 0.030$  and  $0.413 \pm 0.013 \text{ g cm}^{-3}$  after alkali treatment. This increase in BD suggests a reduction in void spaces between fibers due to the removal of impurities like waxes and hemicelluloses, resulting in a more compact fiber structure.<sup>44</sup> True density, on the other hand, showed slight changes for raw areca nut fibers having values of  $4.799 \pm 0.018 \text{ g cm}^{-3}$ , which increased to  $6.308 \pm 0.333 \text{ g cm}^{-3}$  after alkali treatment, while there were no significant changes for the water hyacinth fibers. In addition, the porosity of the fibers decreased post-treatment, with raw areca fibers and water hyacinth fibers initially showing



Table 2 Physical and functional properties of fibers<sup>a</sup>

Parameters	Raw areca nut husk fiber	Alkali-treated areca nut husk fiber	Raw water hyacinth fiber	Alkali-treated water hyacinth fiber
Moisture content (%)	13.191 ± 1.21 <sup>b</sup>	9.432 ± 0.973 <sup>a</sup>	14.760 ± 0.861 <sup>b</sup>	10.540 ± 0.693 <sup>a</sup>
Bulk density (g cm <sup>-3</sup> )	0.137 ± 0.012 <sup>a</sup>	0.828 ± 0.030 <sup>c</sup>	0.159 ± 0.008 <sup>a</sup>	0.413 ± 0.013 <sup>b</sup>
True density (g cm <sup>-3</sup> )	4.799 ± 0.018 <sup>b</sup>	6.308 ± 0.333 <sup>c</sup>	1.583 ± 0.070 <sup>a</sup>	1.813 ± 0.060 <sup>a</sup>
Porosity	0.972 ± 0.002 <sup>d</sup>	0.867 ± 0.002 <sup>b</sup>	0.899 ± 0.004 <sup>c</sup>	0.772 ± 0.014 <sup>a</sup>
Water absorption index (g g <sup>-1</sup> )	8.593 ± 0.769 <sup>b</sup>	6.690 ± 0.324 <sup>a</sup>	10.340 ± 0.333 <sup>c</sup>	6.143 ± 0.409 <sup>a</sup>
Oil absorption index (g g <sup>-1</sup> )	6.251 ± 0.997 <sup>d</sup>	3.237 ± 0.997 <sup>ab</sup>	4.523 ± 0.140 <sup>b</sup>	1.960 ± 0.022 <sup>a</sup>
Water swelling power (g g <sup>-1</sup> )	8.540 ± 0.250 <sup>b</sup>	7.070 ± 0.421 <sup>a</sup>	11.68 ± 0.345 <sup>c</sup>	8.097 ± 0.471 <sup>b</sup>
Oil swelling power (g g <sup>-1</sup> )	8.297 ± 1.034 <sup>c</sup>	7.471 ± 1.563 <sup>c</sup>	4.610 ± 0.102 <sup>b</sup>	2.000 ± 0.095 <sup>a</sup>

<sup>a</sup> Values are mean ± standard deviation. Different lowercase letters in the same row indicate a statistically significant ( $p < 0.05$ ) difference (Duncan's multiple range test).

porosity values of  $0.972 \pm 0.002$  and  $0.899 \pm 0.004$ , reducing to  $0.867 \pm 0.002$  and  $0.772 \pm 0.014$ , respectively. This decrease in porosity can be attributed to the removal of impurities and the filling of gaps between fibers, resulting in a more densely packed fiber structure.

### 3.2. Functional properties of fibers

The functional properties of areca nut husk and water hyacinth fibers, both in their raw form and after alkali treatment, are presented in Table 2. Alkali treatment enhances the fiber's hydrophobic nature by removing lignin and hemicellulose components, thus increasing cellulose content, crystallinity, and surface roughness.<sup>35</sup> The water absorption index (WAI) values for raw areca and water hyacinth fibers were  $8.593 \pm 0.769$  and  $10.340 \pm 0.333$  (g g<sup>-1</sup>), respectively, whereas alkali treatment reduced the WAI to  $6.690 \pm 0.324$  and  $6.143 \pm 0.409$  (g g<sup>-1</sup>), respectively. The WAI was significantly influenced by the alkali treatment ( $p < 0.05$ ), and this decrease indicates a reduction in water uptake, attributed to the removal of hydrophilic components. Furthermore, the reduction in water absorption observed in the alkali-treated fibers is consistent with the results reported in studies on sisal fibers by Sahai *et al.*<sup>75</sup> and *Roystonea regia* fibers by Goud & Rao,<sup>76</sup> indicating a common trend in fiber behaviour post-alkali treatment.

Similarly, the oil absorption index (OAI) decreased significantly ( $p < 0.05$ ) after alkali treatment, with raw areca and water hyacinth fibers having OAI values of  $6.251 \pm 0.997$  and  $4.523 \pm 0.140$  (g g<sup>-1</sup>), respectively, while alkali-treated fibers showed values of  $3.237 \pm 0.997$  and  $1.960 \pm 0.022$  (g g<sup>-1</sup>), respectively. Lower OAI values post-treatment signify reduced oil absorption, correlating with increased hydrophobicity.

Furthermore, the water swelling power (WSP) of both fiber types decreased significantly after treatment ( $p < 0.05$ ), indicating a reduced swelling capacity in water. For raw areca and water hyacinth fibers, the WSP values were  $8.540 \pm 0.250$  and  $11.68 \pm 0.345$  (g g<sup>-1</sup>), respectively, whereas alkali-treated fibers showed values of  $7.070 \pm 0.421$  and  $8.097 \pm 0.471$  (g g<sup>-1</sup>), respectively. Similarly, oil swelling power (OSP) decreased significantly ( $p < 0.05$ ) in alkali-treated water hyacinth fibers, reflecting a reduced oil swelling capacity. However, the OSP of

areca nut fibers didn't show a significant change after alkali treatment.

Overall, these results demonstrate that alkali treatment effectively modifies the functional properties of the fibers, making them suitable for the development of lightweight, high-performance polymer plates.

### 3.3. FTIR analysis of fibers

The FTIR spectral analysis reveals significant alterations in peak positions and intensities between raw and alkali-treated areca nut husk and water hyacinth fibers, indicating the efficacy of alkali treatment in modifying the fiber composition. From Fig. 1, in the raw fibers, characteristic peaks at  $3441\text{ cm}^{-1}$  and  $2923\text{ cm}^{-1}$  are due to the stretching vibrations of O-H and C-H bonds, respectively, indicating the presence of cellulose and hemicellulose components. Peaks at  $2128\text{ cm}^{-1}$  and  $1737\text{ cm}^{-1}$  suggest the presence of lignin, while peaks at  $1656\text{ cm}^{-1}$ ,  $1462\text{ cm}^{-1}$ , and  $1023\text{ cm}^{-1}$  may indicate various functional groups within the fiber structure. However, after alkali treatment, a notable shift is observed in some peaks, such as the

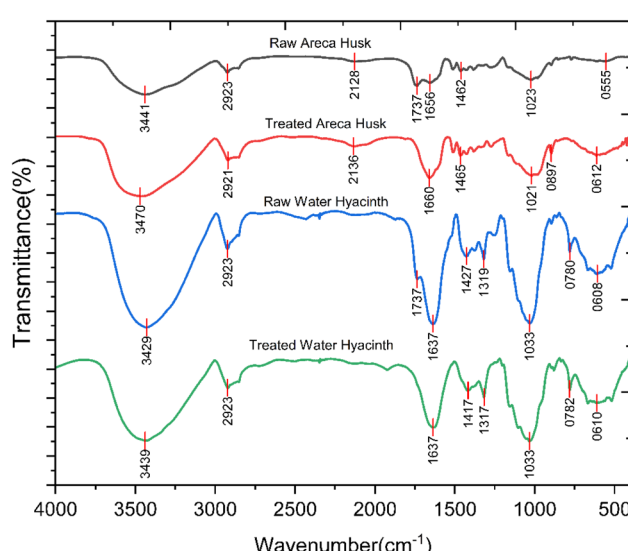


Fig. 1 FTIR spectra of raw and alkali-treated fibers.

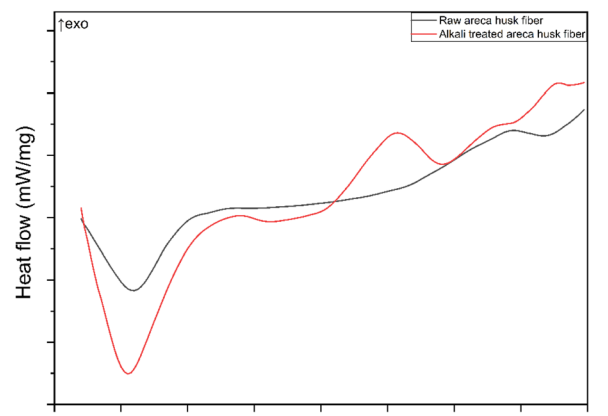


increase in intensity at  $3470\text{ cm}^{-1}$ , indicating an enhanced presence of O-H stretching vibrations due to the removal of hemicellulose. The peak at  $2136\text{ cm}^{-1}$  suggests the partial removal of lignin, corroborated by the decrease in intensity at  $1660\text{ cm}^{-1}$ , associated with lignin's aromatic skeletal vibrations. The reduction in peak intensity at  $1465\text{ cm}^{-1}$  further supports lignin degradation, while the consistent intensity at  $1021\text{ cm}^{-1}$  suggests minimal alteration in cellulose content. The appearance of a new peak at  $897\text{ cm}^{-1}$  in alkali-treated fibers may indicate the presence of alkali-insoluble components, potentially residual lignin. Moreover, a peak at  $612\text{ cm}^{-1}$  suggests changes in crystallinity or structural rearrangements induced by alkali treatment.<sup>35</sup>

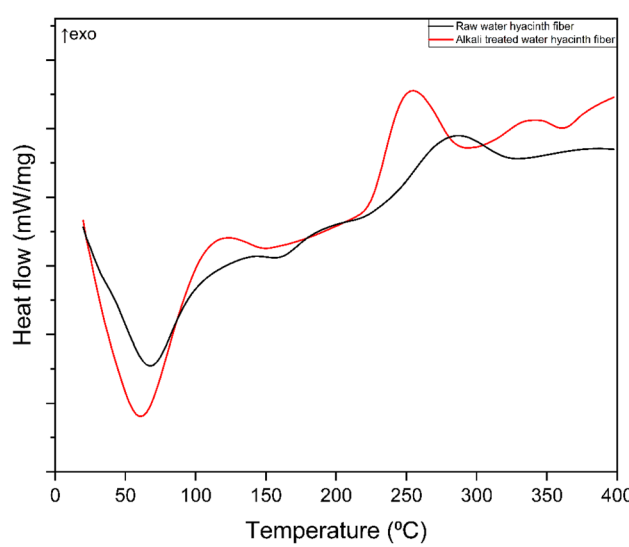
In the case of raw water hyacinth fibers, characteristic peaks at  $3429\text{ cm}^{-1}$  and  $2923\text{ cm}^{-1}$  correspond to O-H and C-H stretching vibrations, respectively, indicative of cellulose and hemicellulose components. Peaks at  $1737\text{ cm}^{-1}$  and  $1637\text{ cm}^{-1}$  suggest the presence of lignin and additional functional groups within the fiber structure. However, after alkali treatment, slight decreases in peak intensities are observed across several bands while the peak positions remain largely unchanged. Specifically, the decrease in intensity at  $1637\text{ cm}^{-1}$  suggests a reduction in lignin content, indicating lignin removal or modification due to alkali treatment. Similarly, the decrease in intensity at  $1417\text{ cm}^{-1}$  also supports lignin degradation, albeit to a lesser extent. Moreover, the small reductions in peak intensities at  $1317\text{ cm}^{-1}$  and  $782\text{ cm}^{-1}$  further suggest alterations in fiber composition, possibly reflecting the removal or modification of hemicellulose components. Interestingly, the peak intensity at  $1033\text{ cm}^{-1}$  remains relatively constant, indicating minimal changes in cellulose content post-alkali treatment. These findings suggest that alkali treatment induces partial removal or modification of hemicellulose and lignin components in areca nut husk and water hyacinth fibers, leading to subtle alterations in fiber composition and potential improvements in fiber properties.<sup>48</sup>

#### 3.4. Thermal analysis of fiber

The DSC analysis shows the impact of alkali treatment on the thermal properties of areca nut husk and water hyacinth fibers. For raw areca nut husk fibers, the DSC curve Fig. 2(a) reveals a broad endothermic peak between 50 and  $80\text{ }^{\circ}\text{C}$ , which corresponds to the evaporation of moisture within the fibers. This is followed by a smaller exothermic peak at around  $340$  to  $360\text{ }^{\circ}\text{C}$  for raw fibers, indicating the thermal degradation of hemicellulose and lignin. The endothermic peak related to water evaporation becomes less pronounced in alkali-treated fibers, reflecting reduced moisture content. In contrast, the alkali-treated fiber displays a sharper exothermic transition beginning near  $250\text{ }^{\circ}\text{C}$ , peaking more distinctly than the raw fiber. This is indicative of a more defined thermal degradation event, primarily associated with cellulose breakdown and partial removal of hemicellulose and lignin, which results in improved fiber crystallinity.<sup>77</sup> Similarly, the DSC curve of water hyacinth fibers in Fig. 2(b) shows a prominent endothermic peak between 50 and  $100\text{ }^{\circ}\text{C}$ , associated with moisture evaporation.



(a)



(b)

Fig. 2 DSC curves of (a) raw and alkali-treated areca nut husk fibers and (b) raw and alkali-treated water hyacinth fibers.

However, the alkali-treated fiber exhibits a sharper exothermic peak at around  $250$  to  $270\text{ }^{\circ}\text{C}$ , suggesting the removal of surface impurities.<sup>77</sup> Similar findings were reported by Lemita *et al.*,<sup>78</sup> where the DSC analysis of *Strelitzia reginae* fibers revealed dehydration peaks below  $100\text{ }^{\circ}\text{C}$  and stability between  $160$  and  $260\text{ }^{\circ}\text{C}$ . Raw fibers showed exothermic peaks at around  $291.4\text{ }^{\circ}\text{C}$  due to hemicellulose degradation. NaOH treatment improved thermal stability by reducing lignin and hemicellulose content.

#### 3.5. Physical and functional properties of biodegradable plates

**3.5.1. Thickness and grammage.** The thickness of the biodegradable plates varied across different compositions of areca nut husk fiber and water hyacinth fiber (Table 3), ranging from  $1.66 \pm 0.19\text{ mm}$  to  $2.05 \pm 0.06\text{ mm}$ . The plate with 100% areca nut husk fiber (C<sub>1</sub>) exhibited the lowest thickness, while



Table 3 Properties of biodegradable plates<sup>a</sup>

Plate number	Thickness (mm)	Grammage (g m <sup>-2</sup> )	Bulk density (g cm <sup>-3</sup> )	Moisture content (%)	Water absorptiveness (g m <sup>-2</sup> )	Absorbency (s)
C <sub>1</sub>	1.66 ± 0.19 <sup>a</sup>	994.33 ± 38.00 <sup>a</sup>	0.127 ± 0.019 <sup>a</sup>	9.27 ± 1.99 <sup>a</sup>	248.00 ± 50.46 <sup>a</sup>	5507.00 ± 202.07 <sup>e</sup>
C <sub>2</sub>	1.68 ± 0.04 <sup>a</sup>	1090.00 ± 13.45 <sup>b</sup>	0.150 ± 0.019 <sup>b</sup>	10.62 ± 0.25 <sup>b</sup>	309.67 ± 55.53 <sup>ab</sup>	4632.00 ± 281.91 <sup>d</sup>
C <sub>3</sub>	1.82 ± 0.05 <sup>ab</sup>	1220.23 ± 23.41 <sup>c</sup>	0.146 ± 0.006 <sup>b</sup>	11.18 ± 0.24 <sup>bc</sup>	388.90 ± 15.50 <sup>bc</sup>	592.33 ± 90.97 <sup>c</sup>
C <sub>4</sub>	1.93 ± 0.06 <sup>bc</sup>	1315.67 ± 20.55 <sup>d</sup>	0.184 ± 0.006 <sup>c</sup>	10.27 ± 0.26 <sup>b</sup>	481.33 ± 61.04 <sup>c</sup>	408.00 ± 17.09 <sup>bc</sup>
C <sub>5</sub>	1.95 ± 0.12 <sup>bc</sup>	1276.00 ± 28.16 <sup>cd</sup>	0.193 ± 0.004 <sup>c</sup>	13.59 ± 0.11 <sup>d</sup>	811.67 ± 45.65 <sup>d</sup>	191.00 ± 52.37 <sup>ab</sup>
C <sub>6</sub>	1.98 ± 0.04 <sup>bc</sup>	1401.67 ± 80.41 <sup>e</sup>	0.196 ± 0.003 <sup>c</sup>	12.85 ± 0.24 <sup>d</sup>	1380.67 ± 117.37 <sup>e</sup>	181.67 ± 14.05 <sup>ab</sup>
C <sub>7</sub>	2.05 ± 0.06 <sup>d</sup>	1483.33 ± 70.78 <sup>f</sup>	0.204 ± 0.005 <sup>c</sup>	12.47 ± 0.35 <sup>cd</sup>	1934.67 ± 113.57 <sup>e</sup>	129.33 ± 15.57 <sup>a</sup>

Color parameters						
Plate number	L*	a*	b*	ΔE	Whiteness index	Tensile strength (MPa)
C <sub>1</sub>	53.05 ± 0.18 <sup>e</sup>	7.03 ± 0.07 <sup>bc</sup>	29.28 ± 0.23 <sup>e</sup>	0.00	44.22 ± 0.06 <sup>e</sup>	3.14 ± 0.13 <sup>b</sup>
C <sub>2</sub>	48.65 ± 0.23 <sup>d</sup>	7.88 ± 0.10 <sup>e</sup>	27.89 ± 1.50 <sup>e</sup>	5.04 ± 0.29 <sup>a</sup>	41.02 ± 0.89 <sup>d</sup>	3.25 ± 0.12 <sup>b</sup>
C <sub>3</sub>	45.09 ± 1.37 <sup>c</sup>	7.70 ± 0.28 <sup>de</sup>	24.16 ± 1.43 <sup>d</sup>	9.83 ± 0.30 <sup>b</sup>	39.52 ± 1.85 <sup>cd</sup>	3.31 ± 0.09 <sup>b</sup>
C <sub>4</sub>	43.93 ± 0.82 <sup>c</sup>	6.83 ± 0.25 <sup>b</sup>	21.37 ± 1.38 <sup>c</sup>	12.33 ± 0.72 <sup>c</sup>	39.60 ± 1.17 <sup>cd</sup>	3.99 ± 0.31 <sup>c</sup>
C <sub>5</sub>	41.59 ± 1.39 <sup>b</sup>	7.42 ± 0.31 <sup>cd</sup>	21.11 ± 0.67 <sup>c</sup>	14.32 ± 0.94 <sup>d</sup>	37.45 ± 1.51 <sup>bc</sup>	3.83 ± 0.28 <sup>c</sup>
C <sub>6</sub>	39.88 ± 1.39 <sup>b</sup>	7.14 ± 0.15 <sup>bc</sup>	17.73 ± 0.78 <sup>b</sup>	17.73 ± 1.50 <sup>e</sup>	36.91 ± 1.15 <sup>b</sup>	3.07 ± 0.33 <sup>b</sup>
C <sub>7</sub>	35.37 ± 1.25 <sup>a</sup>	6.17 ± 0.34 <sup>a</sup>	12.99 ± 1.19 <sup>a</sup>	24.30 ± 0.67 <sup>f</sup>	33.78 ± 1.42 <sup>a</sup>	2.53 ± 0.14 <sup>a</sup>

<sup>a</sup> Values are mean ± standard deviation. Different lowercase letters in the same column indicate a statistically significant ( $p < 0.05$ ) difference (Duncan's multiple range test).

the plate with 100% water hyacinth fiber (C<sub>7</sub>) showed the highest thickness. As the proportion of water hyacinth fiber increased in the plate, there was a trend of increasing thickness and a significant difference among the composites ( $p < 0.05$ ). This variation in thickness can be attributed to the differing structural properties and binding capacities of the fibers within the plates. These findings suggest that the composition of the fibers significantly influences the thickness of the resulting plate material. Additionally, similar to the study by Machado *et al.*,<sup>79</sup> where foam thickness was significantly affected by the sesame residue concentration, the results underscore the role of fiber composition in determining the physical characteristics of the plate material.

The grammage of the biodegradable plates exhibited variations corresponding to different compositions of areca nut husk and water hyacinth fibers (Table 3). The grammage values ranged from 994.33 ± 38.00 g m<sup>-2</sup> for plate C<sub>1</sub> (100% areca nut husk fiber) to 1483.33 ± 70.78 g m<sup>-2</sup> for plate C<sub>7</sub> (100% water hyacinth fiber). These values represent a gradual increase in mass per unit area as the proportion of water hyacinth fiber in the plate increased ( $p < 0.05$ ). Such variations in grammage are indicative of changes in the density and compactness of the plate materials. As discussed by Iewkittayakorn *et al.*,<sup>64</sup> variations in grammage can influence the thickness of paper products, indicating potential implications for the thickness of these biodegradable plates. Higher grammage increases transportation weight, which leads to higher logistics costs and reduced load capacity, along with more storage, handling, and environmental impacts.<sup>3</sup> The observed differences in grammage among the plate formulations in this study may also reflect variations in plate thickness, alongside other physical

properties, influenced by the composition of areca nut husk and water hyacinth fibers.

**3.5.2. Bulk density.** The bulk density (g cm<sup>-3</sup>) of the biodegradable plates with varying fiber ratios (C<sub>1</sub> to C<sub>7</sub>) was analyzed to understand the impact of fiber composition on the density of the resulting plates. The findings (Table 3) reveal a notable variation in BD across different compositions, ranging from 0.127 ± 0.019 to 0.204 ± 0.005 g cm<sup>-3</sup>, but there was no significant difference observed in the values after composition C<sub>4</sub> ( $p \geq 0.05$ ). The observed trend suggests that as the proportion of water hyacinth fiber increases relative to areca nut husk fiber, there is a tendency for the BD to increase. This may be due to the addition of water hyacinth fiber; the viscosity of the starch batter has increased, consequently restraining the expansion of steam bubbles while foaming.<sup>43</sup> This led to the formation of starch foams with reduced cell size and increased densities. This trend can be attributed to the water hyacinth fiber potentially filling up the voids between the matrix of areca fiber and starch. This phenomenon represents the role of fiber interactions within the plate matrix in influencing its density characteristics. The densities observed in this study were lower compared to those documented by Mello *et al.*<sup>80</sup> for cassava starch foams created using malt bagasse (ranging from 0.415 to 0.450 g cm<sup>-3</sup>). However, they were comparable, or marginally higher in certain compositions, to the densities reported by Kaisangsri *et al.*<sup>65</sup> for foam trays fabricated from cassava starch blended with natural fiber and chitosan (0.120–0.140 g cm<sup>-3</sup>).

**3.5.3. Moisture content.** The moisture content (MC) of the biodegradable plates varied significantly ( $p < 0.05$ ) with the composition of areca nut husk fiber and water hyacinth fiber. As illustrated in Table 3, the MC of the plates ranged from 9.27 ±



1.99 to  $13.59 \pm 0.11\%$ . Specifically, plates with higher proportions of water hyacinth fiber exhibited increased MC, with plate C<sub>5</sub> having the highest MC of  $13.59 \pm 0.11\%$ , while plate C<sub>1</sub> with 100% areca nut husk fiber had the lowest MC of  $9.27 \pm 1.99\%$ . This trend suggests that the incorporation of water hyacinth fiber influences moisture absorption in the plates. Previous studies have indicated similar trends, where the addition of fillers reduced MC initially due to the optimum fibers as fillers presented in the tortuous path for water molecules. However, at higher loading levels of water hyacinth fiber, the MC slightly increased. This phenomenon is associated with the presence of free -OH groups in agglomerations of water hyacinth fiber within the starch matrix, facilitating interactions with water molecules.<sup>43</sup> Structurally, a higher amount of water hyacinth fibers may create micro-voids or channels within the matrix, allowing water to occupy these spaces and further enhancing the moisture content of the plates.<sup>81</sup>

**3.5.4. Water absorptiveness.** The water absorptiveness of the biodegradable plates developed using different compositions of areca nut husk fiber and water hyacinth fiber (C<sub>1</sub> to C<sub>7</sub>) exhibited varying levels of water uptake (Table 3). The water absorptiveness increased with higher proportions of water hyacinth fiber in the plate, and the values were significantly different from each other ( $p < 0.05$ ). Specifically, plates with higher water hyacinth fiber content, such as C<sub>6</sub> and C<sub>7</sub>, displayed significantly higher water absorptiveness,  $1380.67 \pm 117.37 \text{ g m}^{-2}$  and  $1934.67 \pm 113.57 \text{ g m}^{-2}$ , compared to those with lower water hyacinth fiber content. This suggests that incorporating water hyacinth fiber enhances the plate's water absorption capacity, likely due to altered interaction with the starch matrix beyond a certain threshold of the water hyacinth fiber concentration.<sup>82</sup> However, high water absorptiveness can negatively affect food applications by causing plates to soften, lose mechanical strength, or allow leakage when holding moist or oily foods.<sup>83,84</sup>

**3.5.5. Absorbency.** The water absorbency exhibited a statistically significant ( $p < 0.05$ ) variation across the compositions (Table 3). The highest absorbency was observed in the C<sub>1</sub> composition ( $5507.00 \pm 202.07 \text{ s}$ ), followed by C<sub>2</sub> ( $4632.00 \pm 281.91 \text{ s}$ ), indicating a decreasing trend with the incorporation of water hyacinth fiber. The absorbency significantly decreased as the proportion of water hyacinth fiber increased, with C<sub>7</sub> showing the lowest absorbency ( $129.33 \pm 15.57 \text{ s}$ ). This trend suggests that the water absorbency of the plates is influenced by the ratio of areca to water hyacinth fibers, with higher proportions of areca fiber leading to greater absorbency. Harikrishnan *et al.*<sup>85</sup> reported that the interaction of the composite with water varies depending on the type of fiber added. This variation among samples may be due to compositional differences, interactions between fibers and other reinforcing or binding agents, the porosity of the samples, and the structure of the fibers.

**3.5.6. Measurement of color.** Assessing the color of plates is crucial not only for aesthetic reasons but also to detect any potential degradation. The findings reveal that the fiber content significantly impacts the color of the plates (Table 3). Specifically, the lightness ( $L^*$ ) and whiteness index decreased as the

areca nut husk fiber content decreased and the water hyacinth fiber content increased, ranging from  $53.05 \pm 0.18$  to  $35.37 \pm 1.25$  and  $44.22 \pm 0.06$  to  $33.78 \pm 1.42$ , respectively. Plates with higher water hyacinth content exhibited lower lightness and were significantly different ( $p < 0.05$ ) for each composition. The variation in the  $a^*$  value was less, ranging from  $6.17 \pm 0.34$  to  $7.88 \pm 0.10$  across different fiber concentrations, suggesting a minimal influence on the plates' redness by fiber content. Conversely, the  $b^*$  value, reflecting yellowness and blueness, decreased from  $29.28 \pm 0.23$  to  $12.99 \pm 1.19$  with decreasing areca nut husk fiber content and increasing water hyacinth fiber content, suggesting a bluish effect on the plate, and there was a significant difference ( $p < 0.05$ ) among the compositions. The reduction in luminosity, combined with the increase in the  $b^*$  parameter, led to a statistically significant ( $p < 0.05$ ) higher color total difference ( $\Delta E$ ) compared to plates with 100% areca nut husk fiber. These color variations may stem from the inherent color of the added fibers and the high temperatures employed in the process, potentially associated with Maillard reactions due to the high carbohydrate content in the raw materials.<sup>79</sup>

**3.5.7. Mechanical properties.** According to Salgado *et al.*,<sup>86</sup> the stress and strain values at the fracture point are key properties to assess the plates for their suitability in various applications. In the present study, the TS of biodegradable foam plates prepared from various fiber compositions is reported in Table 3. The TS of the plates increased from the composition C<sub>1</sub> to C<sub>4</sub>, rising from  $3.14 \pm 0.13 \text{ MPa}$  to  $3.99 \pm 0.31 \text{ MPa}$ . Conversely, when the areca nut husk fiber content was further reduced and replaced with higher proportions of water hyacinth (C<sub>5</sub> to C<sub>7</sub>), the TS of the plates began to decline from  $3.83 \pm 0.28 \text{ MPa}$  to  $2.53 \pm 0.14 \text{ MPa}$ . Statistical analysis confirmed that the differences in the TS among these compositions were significant ( $P < 0.05$ ). Among the tested formulations, composition C<sub>4</sub> (50% areca nut husk fiber and 50% water hyacinth fiber) exhibited the highest TS. This improvement was due to the moderate incorporation of water hyacinth fiber enhancing the mechanical strength up to a certain threshold; beyond a certain threshold, excess fiber disrupts the interaction of fiber and the other components of the matrix, thereby reducing mechanical strength.<sup>65</sup> In addition, the hydrogen bonding interactions between hydroxyl groups of starch and cellulose fiber likely contributed to the improved matrix-fiber adhesion and mechanical strength.<sup>87</sup> Furthermore, the variation in the TS among various compositions may be associated with additional factors such as surface polarity, mechanical interlocking, and roughness, which influence the interaction between the fiber and matrix.<sup>85</sup> When compared with earlier studies, the foam plates developed in the present study demonstrated remarkable TS. For example, foams produced from cross-linked corn starch reinforced with corn husk fiber, kaolin, and beeswax exhibited TS values between 1.06 MPa and 1.67 MPa, while commercial expanded polystyrene (EPS) foams showed around 1.1 MPa. In contrast, the TS values obtained in the present study were more aligned with those in the previous study on starch-based foams reinforced with banana bunch stalk fibers (2.4 MPa to 3.7 MPa), respectively.<sup>54</sup>



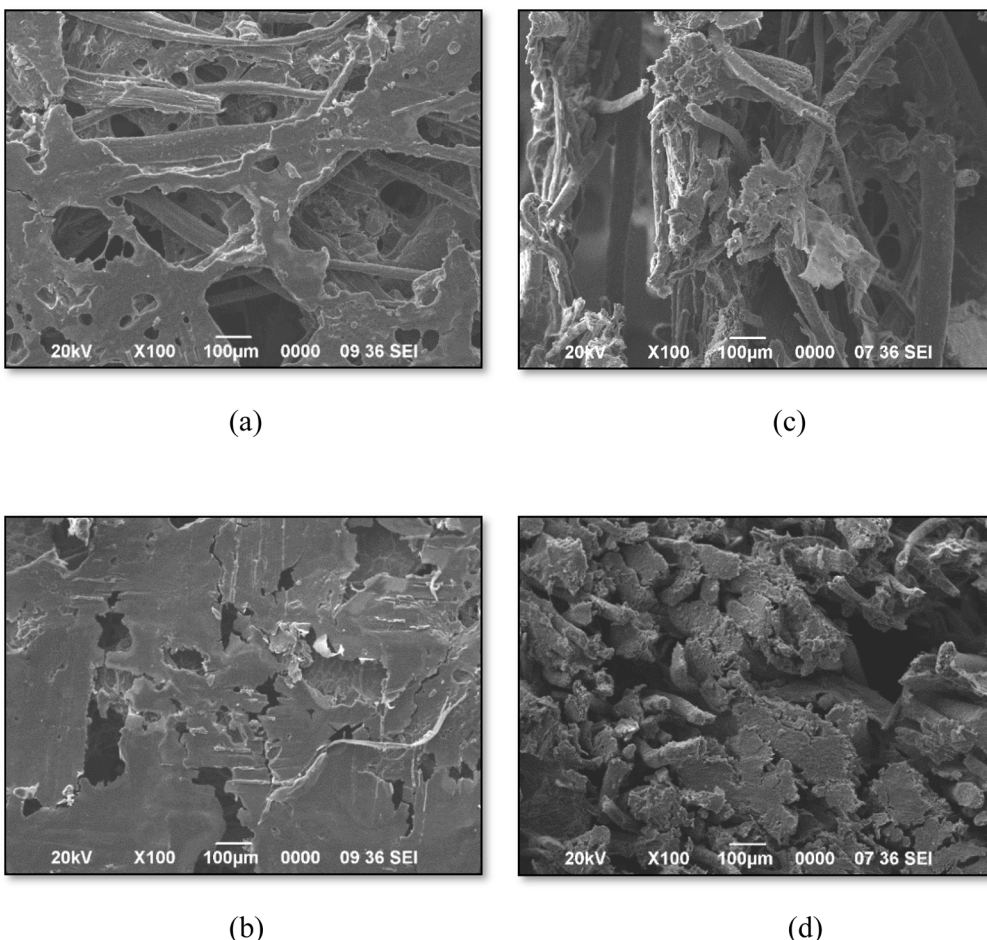


Fig. 3 SEM images of the plate surface (a) with 100% areca nut husk fiber, (b) with 50% fibers from areca nut husk and 50% fibers from water hyacinth; SEM images of the cross-section of plates (c) with 100% areca nut husk, (d) with 50% fibers from areca nut husk and 50% fibers from water hyacinth (magnifications: 100×).

**3.5.8. Morphological analysis.** The morphology of the surface and cross-sectional area of the biodegradable plates is shown in Fig. 3. Notably, the composite surface exhibited enhanced homogeneity after incorporating both types of fibers. However, the plates with only areca fiber showed void spaces within the matrix, which may be filled by the water hyacinth fiber. Therefore, the water hyacinth fiber also acts as a filler within the matrix, enhancing properties such as physical and mechanical strength. This indicates the good dispersion of both areca nut husk and water hyacinth fibers within the matrix.

### 3.6. Hydrophobic coating of the selected plate with optimal composition

The optimal composition was chosen based on some key desirability aspects, such as lower BD (to reduce material handling costs), lower MC (to enhance product stability), and acceptable thickness, water absorptiveness, absorbency, TS, and visual appearance.<sup>61</sup> According to the analysis of the desirable parameters for biodegradable plates, the combination C<sub>4</sub> emerged as the optimal formulation for developing biodegradable composite plates. This specific blend was selected as

the best proportion of fiber for applying a waterproof coating to improve the resistance of the plate against moisture. Consequently, the optimized biodegradable composite plate, coated with beeswax, is illustrated in Fig. 4. The beeswax-coated plates had a uniform, glossy finish and natural tone, which improves their aesthetic and functional appeal for food contact applications.

**3.6.1. Properties of the coated plates.** The application of beeswax coating significantly enhanced several properties of the biodegradable plates, as illustrated in Table 4. Although there was no statistically significant difference in thickness and bulk density (BD) between coated and uncoated samples ( $p \geq 0.05$ ), a significant ( $p < 0.05$ ) increase in grammage was observed in the coated plates ( $1537 \pm 35.78 \text{ g m}^{-2}$ ) compared to the uncoated ones ( $1315.67 \pm 20.55 \text{ g m}^{-2}$ ), which indicates effective deposition of beeswax on the surface of the plates. Therefore, the amount of coating applied on the plate surface was  $\sim 221 \text{ g m}^{-2}$  (difference in grammage after and before coating). The coating exhibited excellent hydrophobicity, as shown by a significant ( $p < 0.05$ ) reduction in water absorptiveness from  $481.33 \pm 61.04$  to  $57 \pm 9.07 \text{ g m}^{-2}$  and water solubility from



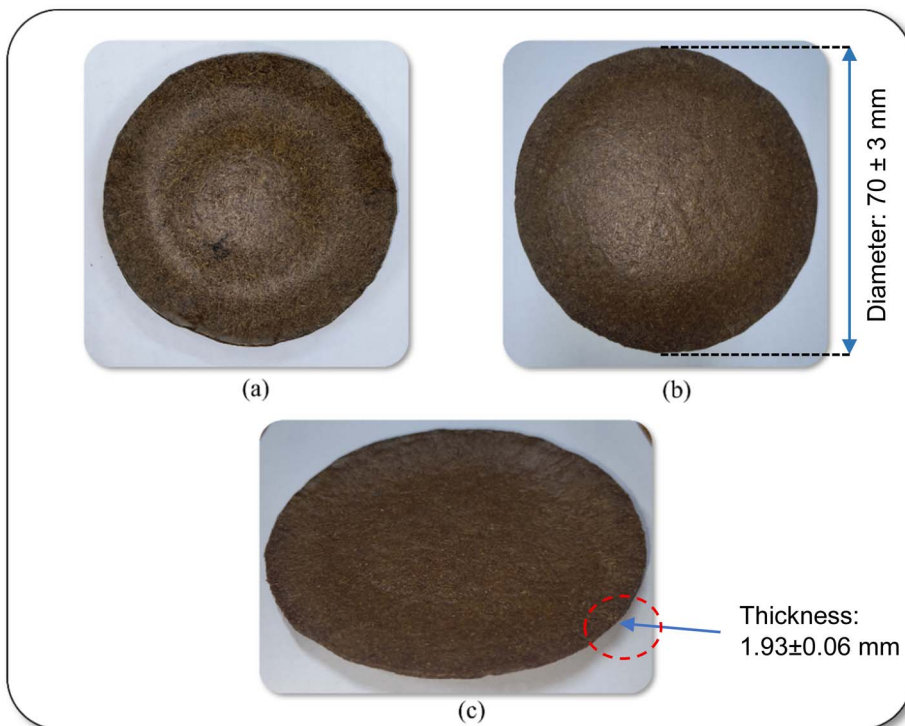


Fig. 4 Visual appearance of the plate with final composition (C<sub>4</sub>) after coating. (a) Top view, (b) bottom view, and (c) side view.

Table 4 Properties of the selected plate after coating<sup>a</sup>

Sample/parameters	Without coating	With coating
Thickness (mm)	1.93 ± 0.06 <sup>a</sup>	2.01 ± 0.16 <sup>a</sup>
Grammage (g m <sup>-2</sup> )	1315.67 ± 20.55 <sup>a</sup>	1537 ± 35.78 <sup>b</sup>
Bulk density (g cm <sup>-3</sup> )	0.184 ± 0.01 <sup>a</sup>	0.22 ± 0.08 <sup>a</sup>
Water absorptiveness (g m <sup>-2</sup> )	481.33 ± 61.04 <sup>a</sup>	57 ± 9.07 <sup>b</sup>
Absorbency (S)	408.00 ± 17.09 <sup>a</sup>	>5000 <sup>b</sup>
Water solubility (%)	25.43 ± 3.11 <sup>a</sup>	5.32 ± 1.09 <sup>b</sup>
Color parameters		
<i>L</i> *	43.93 ± 0.82 <sup>a</sup>	38.92 ± 0.81 <sup>b</sup>
<i>a</i> *	6.83 ± 0.25 <sup>a</sup>	6.76 ± 0.05 <sup>a</sup>
<i>b</i> *	21.37 ± 1.38 <sup>a</sup>	16.71 ± 0.29 <sup>b</sup>
Δ <i>E</i>	12.33 ± 0.72 <sup>a</sup>	14.14 ± 0.67 <sup>b</sup>
Whiteness index	39.60 ± 1.17 <sup>a</sup>	36.31 ± 0.57 <sup>a</sup>
Tensile strength (MPa)	3.99 ± 0.31 <sup>a</sup>	5.01 ± 0.42 <sup>b</sup>

<sup>a</sup> Values are mean ± standard deviation. Different lowercase letters in the same row indicate a statistically significant (*p* < 0.05) difference.

25.43 ± 3.11% to 5.32 ± 1.09%. Additionally, absorbency was markedly enhanced, increasing from 408.00 ± 17.09 s in the uncoated plate to beyond 5000 s in the beeswax-coated plates, signifying a substantial improvement in moisture barrier performance. In terms of color properties, significant (*p* < 0.05) decreases were noted in lightness and yellowness, along with a noticeable increase in total color difference ( $\Delta E$ : 12.33 ± 0.72 to 14.14 ± 0.67), indicating perceptible visual changes due to the natural tone of beeswax. No significant differences (*p* ≥ 0.05) were observed in *a*\* values and the whiteness index. Mechanically, the TS significantly improved from 3.99 ± 0.31 MPa to 5.01 ± 0.42 MPa. Therefore, beeswax adds a reinforcing layer on the surface, reduces microcrack propagation,

and improves stress distribution, thereby enhancing mechanical integrity.<sup>43,60,61</sup> Similar findings were reported by Iewkit-tayakorn *et al.*<sup>64</sup> for the application of bio-coatings, which have increased both the grammage and thickness of pineapple leaf pulp paper, though this also led to a decrease in density compared to uncoated paper. Among the tested coatings, the beeswax-chitosan solution provided the best water resistance, followed by alginate/gellan gum, chitosan, beeswax, and shellac. Additionally, the beeswax-chitosan coating significantly improved the paper's TS, reaching up to 5.9 kN m<sup>-2</sup>. Therefore, the hydrophobic coatings effectively enhance the water resistance and mechanical strength of the biodegradable plates, making them more suitable for food packaging or serving applications.

### 3.7. Biodegradability test

The visual signs and the mass loss of the plates (with and without coating) during the 6 weeks of biodegradation progression are illustrated in Fig. 5 and 6, respectively. From Fig. 6, it was observed that the overall mass loss of plates was higher in soil compared to sand. In addition, non-coated plates degraded more quickly than coated ones, which suggests that coating the plates with beeswax served as a barrier. This barrier restricts the contact of moisture, microbes, and other factors (oxygen and enzymes) with the underlying components of the plate matrix and delays the degradation process.

During the biodegradability study, the non-coated samples showed a substantial mass loss of nearly 70% in soil and 60% in sand within just four weeks. By the end of this period, the plates had developed cracks and started disintegrating, making it

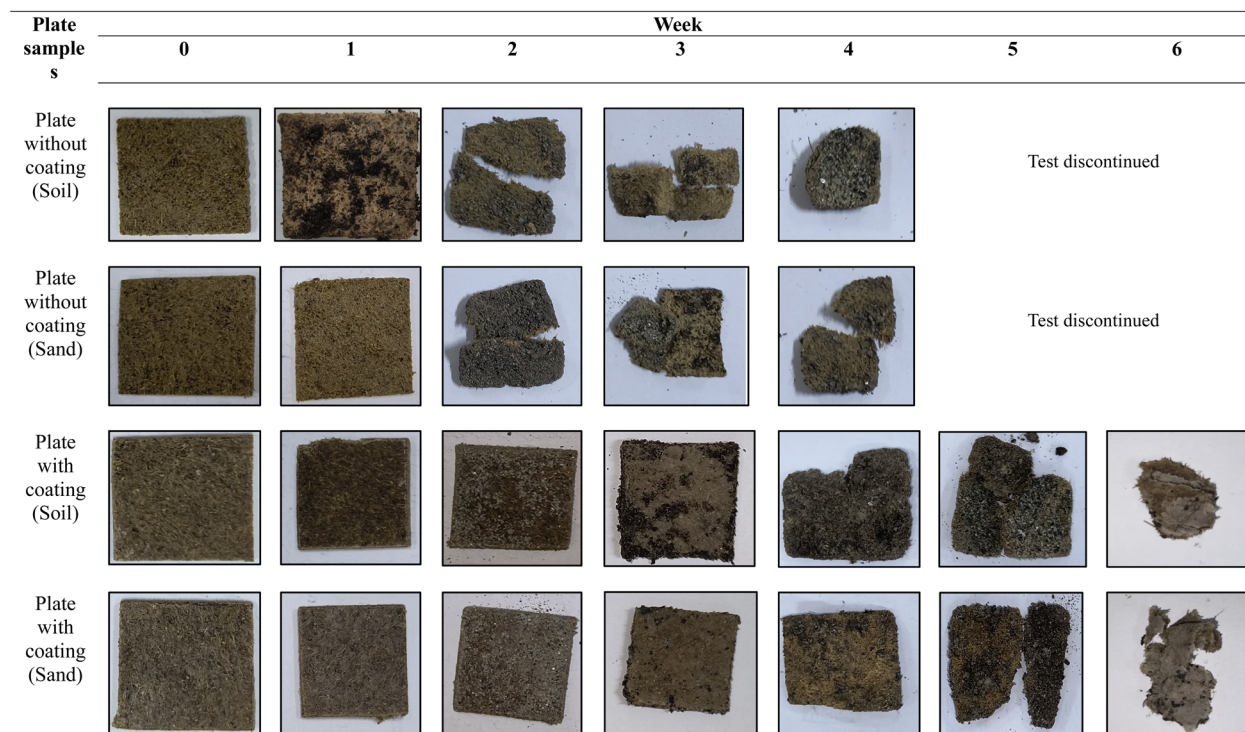


Fig. 5 Visual signs of biodegradation of the plate samples.

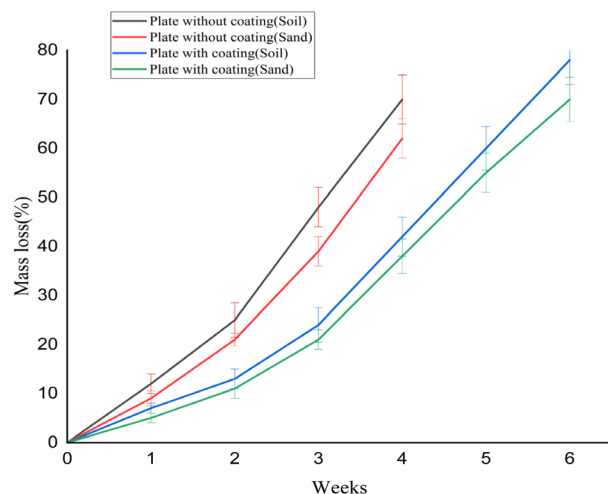


Fig. 6 Biodegradability analysis of coated and non-coated plates.

impractical to continue measurements. As a result, testing of non-coated plates was discontinued beyond the fourth week. In contrast, the coated samples exhibited a relatively slower degradation pattern. Over a six-week period, they showed mass losses of about 75% in soil and 70% in sand, indicating that although coating provided some delay, the material was still significantly biodegradable over time. The primary mechanism for starch biodegradation involves the enzymatic hydrolysis of the polymer chains, resulting in the cleavage of the  $\alpha$ -1,4 bonds in the linear chains of amylose and amylopectin.<sup>71</sup>

Furthermore, the atmospheric heat and activity of microorganisms present in the soil contribute to the degradation process by shortening and weakening the polymer chains of the starch.<sup>88</sup> Biodegradation involves diverse microorganisms (such as cellulolytic, hemicellulolytic, pectinolytic, and lignolytic types), which break down biopolymers and convert their carbon into  $\text{CO}_2$  and restore the carbon cycle.<sup>54,89</sup> Additionally, daily spraying of water may have interacted with the OH groups present in the starch, due to which the chains got weakened and accelerated the process of biodegradation. During this process, the molecular interaction among the starch molecules was likely to be disrupted, resulting in the observable degradation of the polymer matrix.<sup>90</sup> Consequently, the study shows that the prepared plates can easily be disposed of in gardens and flowerbeds, offering an environmentally friendly solution that reduces pollution from plastic materials and lowers the processing costs from the waste of their disposal, as observed by Sanhawong *et al.*<sup>91</sup>

A previous study examined the biodegradation behaviour of corn starch-based foam plates reinforced with banana bunch stalk fibers when buried in both soil and sand for a period of five weeks. The results revealed that samples degraded more rapidly in soil than in sand, as indicated by the higher mass loss in soil. The effect of beeswax coating on the biodegradation process was also reported. Specifically, uncoated plates lost 51.7% of their mass in soil and 43.54% in sand, whereas beeswax-coated plates exhibited lower mass losses of 35.70% in soil and 18.81% in sand.<sup>54</sup> In parallel, another study on sugarcane bagasse-based casings reported a similar trend, with approximately 50% mass loss over five weeks. In contrast, commercial expanded polystyrene (EPS) plates showed negligible changes in their mass under the same conditions.<sup>92</sup>



## 4. Conclusions

The study investigates the development of biodegradable plates made from cellulose fibers sourced from areca nut husk and water hyacinth, bound with tapioca starch. Alkali treatment improved the properties of the fibers, such as physical, functional, and thermal properties. A composite dough was formulated using gelatinized tapioca starch, guar gum, and glycerol, incorporating fibers in various ratios. The optimal composition, C<sub>4</sub> (a 50 : 50 ratio of areca nut husk to water hyacinth fiber), exhibited favorable properties including thickness, density, moisture content, water absorptiveness, and tensile strength. Increasing water hyacinth content negatively impacted the plate's hydrophilicity and mechanical strength. To improve the susceptibility against moisture, the plate with optimal composition was coated with beeswax to make it suitable for foods with low and intermediate moisture content. The coated plates demonstrated superior water resistance, positioning them as viable alternatives to expanded polystyrene (EPS) plates and contributing to the reduction of plastic waste. Biodegradability tests revealed that non-coated plates degraded rapidly in both soil and sand environments, with a significant mass loss observed within weeks. Potential challenges in commercial scaling of the plate may include ensuring long-term mold reuse under repeated heating cycles, which could affect consistency and production efficiency. Another concern is the relatively higher cost of beeswax as a coating material when compared to synthetic hydrophobic alternatives. Future work could explore alternative low-cost coatings and the development of automated and high-throughput molding processes to enhance economic feasibility.

## Ethical review

This study does not involve any human or animal testing.

## Author contributions

Bedanta Rajbongshi: data curation, formal analysis, investigation; writing – original draft; Akuleti Saikumar: methodology, formal analysis, resources; writing – review & editing. Laxmikant S. Badwaik: conceptualization, project administration, resources, supervision, writing – review & editing.

## Conflicts of interest

The authors have declared that there is no conflict of interest for this work.

## Data availability

The data supporting this article have been included within the article.

## Acknowledgements

The authors are thankful for the support received from DST-FIST and UGC-SAP for carrying out the work.

## References

- 1 M. Kan and S. A. Miller, Environmental impacts of plastic packaging of food products, *Resour. Conserv. Recycl.*, 2022, **180**, 106156, DOI: [10.1016/j.resconrec.2022.106156](https://doi.org/10.1016/j.resconrec.2022.106156).
- 2 H. Gupta, H. Kumar and A. K. Gehlaut, Preparation and characterization of bio-composite films obtained from coconut coir and groundnut shell for food packaging, *J. Mater. Cycles Waste Manag.*, 2022, **24**, 569–581, DOI: [10.1007/s10163-021-01343-z](https://doi.org/10.1007/s10163-021-01343-z).
- 3 L. K. Ncube, A. U. Ude, E. N. Ogunmuyiwa, R. Zulkifli and I. N. Beas, Environmental impact of food packaging materials: A review of contemporary development from conventional plastics to polylactic acid based materials, *Materials*, 2020, **13**, 4994, DOI: [10.3390/ma13214994](https://doi.org/10.3390/ma13214994).
- 4 G. Mäder, N. Rüegg, T. Tschichold and S. Yildirim, Utilizing spent coffee grounds as sustainable fillers in biopolymer composites: influence of particle size and content, *Sustainable Food Technol.*, 2025, **3**, 1151–1163, DOI: [10.1039/D5FB00187K](https://doi.org/10.1039/D5FB00187K).
- 5 S. Polat, M.-K. Uslu, A. Aygün and M. Certel, The effects of the addition of corn husk fibre, kaolin and beeswax on cross-linked corn starch foam, *J. Food Eng.*, 2013, **116**, 267–276, DOI: [10.1016/j.jfoodeng.2012.12.017](https://doi.org/10.1016/j.jfoodeng.2012.12.017).
- 6 J. Wang, M. Euring, K. Ostendorf and K. Zhang, Biobased materials for food packaging, *J. Bioresour. Bioprod.*, 2022, **7**, 1–13, DOI: [10.1016/j.jobab.2021.11.004](https://doi.org/10.1016/j.jobab.2021.11.004).
- 7 S. Paudel, S. Regmi, S. Bhattarai, A. Fennell and S. Janaswamy, Valorization of grapevine agricultural waste into transparent and high-strength biodegradable films for sustainable packaging, *Sustainable Food Technol.*, 2025, **3**, 1218–1231, DOI: [10.1039/D5FB00211G](https://doi.org/10.1039/D5FB00211G).
- 8 H. Pulikkalparambil, S. A. Varghese, V. Chonhencob, T. Nampitch, L. Jarupan and N. Harnkarnsujarit, Recent advances in natural fibre-based materials for food packaging applications, *Polymers*, 2023, **15**, 1393, DOI: [10.3390/polym15061393](https://doi.org/10.3390/polym15061393).
- 9 V. Fiore, G. Di Bella and A. Valenza, The effect of alkaline treatment on mechanical properties of kenaf fibers and their epoxy composites, *Composites, Part B*, 2015, **68**, 14–21, DOI: [10.1016/j.compositesb.2014.08.025](https://doi.org/10.1016/j.compositesb.2014.08.025).
- 10 R. Punyamurthy, D. Sampathkumar, R. P. G. Ranganagowda, B. Bennehalli and C. V. Srinivasa, Mechanical properties of abaca fiber reinforced polypropylene composites: Effect of chemical treatment by benzenediazonium chloride, *J. King Saud Univ. Eng. Sci.*, 2017, **29**, 289–294, DOI: [10.1016/j.jksues.2015.10.004](https://doi.org/10.1016/j.jksues.2015.10.004).
- 11 C. Sawsen, K. Fouzia, B. Mohamed and G. Moussa, Effect of flax fibers treatments on the rheological and the mechanical behavior of a cement composite, *Constr. Build. Mater.*, 2015, **79**, 229–235, DOI: [10.1016/j.conbuildmat.2014.12.091](https://doi.org/10.1016/j.conbuildmat.2014.12.091).



12 B. F. Yousif, A. Shalwan, C. W. Chin and K. C. Ming, Flexural properties of treated and untreated kenaf/epoxy composites, *Mater. Des.*, 2012, **40**, 378–385, DOI: [10.1016/j.matdes.2012.04.017](https://doi.org/10.1016/j.matdes.2012.04.017).

13 F. Jahan and M. Soni, Effects of chemical treatment on mechanical properties of various natural fiber reinforced composite: a review, *Mater. Today Proc.*, 2021, **46**, 6708–6711, DOI: [10.1016/j.matpr.2021.04.175](https://doi.org/10.1016/j.matpr.2021.04.175).

14 R. Sukmawan, K. Kusmono and M. W. Wildan, Study of alkali and acetylation treatments on sisal fibers compatibility with low-amine/epoxy stoichiometric ratio, *Results Eng.*, 2024, **24**, 103127, DOI: [10.1016/j.rineng.2024.103127](https://doi.org/10.1016/j.rineng.2024.103127).

15 M. M. Kabir, H. Wang, K. T. Lau, F. Cardona and T. Aravinthan, Mechanical properties of chemically-treated hemp fibre reinforced sandwich composites, *Composites, Part B*, 2012, **43**, 159–169, DOI: [10.1016/j.compositesb.2011.06.003](https://doi.org/10.1016/j.compositesb.2011.06.003).

16 M. P. Harikrishnan, R. Raghunathan, A. S. Warrier, M. Basil, S. K. Sahoo, R. Pandiselvam, T. Venkatesh, S. Pillai, P. Kundu and A. Kothakota, Reinforced water hyacinth based biodegradable cutlery: Green alternative to single-use plastics, *Food Packag. Shelf Life*, 2023, **40**, 101211, DOI: [10.1016/j.fpsl.2023.101211](https://doi.org/10.1016/j.fpsl.2023.101211).

17 P. S. Deshmukh, P. G. Patil, P. U. Shahare, G. B. Bhanage, J. S. Dhekale, K. G. Dhande and V. V. Aware, Effect of mechanical and chemical treatments of arecanut (Areca catechu L.) fruit husk on husk and its fibre, *Waste Manage.*, 2019, **95**, 458–465, DOI: [10.1016/j.wasman.2019.06.026](https://doi.org/10.1016/j.wasman.2019.06.026).

18 UN Food and Agriculture Organization, FAOSTAT, Production/Yield quantities of Areca nuts in World, 2023, <https://www.fao.org/faostat/en/#data/QCL/visualize>, accessed 21 August 2025.

19 L. Yusriah, S. M. Sapuan, E. S. Zainudin and M. Mariatti, Characterization of physical, mechanical, thermal and morphological properties of agro-waste betel nut (Areca catechu) husk fibre, *J. Clean. Prod.*, 2014, **72**, 174–180, DOI: [10.1016/j.jclepro.2014.02.025](https://doi.org/10.1016/j.jclepro.2014.02.025).

20 J. Yuan, H. Zhang, H. Zhao, H. Ren and H. Zhai, Study on dissociation and chemical structural characteristics of areca nut husk, *Molecules*, 2023, **28**, 1513, DOI: [10.3390/molecules28031513](https://doi.org/10.3390/molecules28031513).

21 A. Rajan, J. G. Kurup and T. E. Abraham, Biosoftening of arecanut fiber for value added products, *Biochem. Eng. J.*, 2005, **25**, 237–242, DOI: [10.1016/j.bej.2005.05.011](https://doi.org/10.1016/j.bej.2005.05.011).

22 G. Sunny and T. P. Rajan, Review on areca nut fiber and its implementation in sustainable products development, *J. Nat. Fibers*, 2021, **19**, 4747–4760, DOI: [10.1080/15440478.2020.1870623](https://doi.org/10.1080/15440478.2020.1870623).

23 Z. Ismail, S. Z. Othman, K. H. Law, A. H. Sulaiman and R. Hashim, Comparative Performance of Water Hyacinth (*Eichhornia crassipes*) and Water Lettuce (*Pista stratiotes*) in Preventing Nutrients Build-up in Municipal Wastewater, *Clean: Soil, Air, Water*, 2015, **43**, 521–531, DOI: [10.1002/clen.201200254](https://doi.org/10.1002/clen.201200254).

24 W. Feng, K. Xiao, W. Zhou, D. Zhu, Y. Zhou, Y. Yuan, N. Xiao, X. Wan, Y. Hua and J. Zhao, Analysis of utilization technologies for *Eichhornia crassipes* biomass harvested after restoration of wastewater, *Bioresour. Technol.*, 2017, **223**, 287–295, DOI: [10.1016/j.biortech.2016.10.047](https://doi.org/10.1016/j.biortech.2016.10.047).

25 A. G. Bayrakci and G. Koçar, Second-generation bioethanol production from water hyacinth and duckweed in Izmir: a case study, *Renew. Sustain. Energy Rev.*, 2014, **30**, 306–316, DOI: [10.1016/j.rser.2013.10.011](https://doi.org/10.1016/j.rser.2013.10.011).

26 G. D. O. Okwadha and D. M. Makomele, Evaluation of water hyacinth extract as an admixture in concrete production, *J. Build. Eng.*, 2018, **16**, 129–133, DOI: [10.1016/j.jobe.2018.01.002](https://doi.org/10.1016/j.jobe.2018.01.002).

27 V. B. Barua and A. S. Kalamdhad, Water hyacinth to biogas: a review, *Pollut. Res.*, 2016, **35**, 491–501.

28 P. Priya, S. O. Nikhitha, C. Anand, R. S. Dipin Nath and B. Krishnakumar, Biomethanation of water hyacinth biomass, *Bioresour. Technol.*, 2018, **255**, 288–292, DOI: [10.1016/j.biortech.2018.01.119](https://doi.org/10.1016/j.biortech.2018.01.119).

29 V. D. Tobias, J. L. Conrad and B. Mahardja, Impacts of water hyacinth treatment on water quality in a tidal estuarine environment, *Biol. Invasions*, 2019, **21**, 3479–3490, DOI: [10.1007/s10530-019-02061-2](https://doi.org/10.1007/s10530-019-02061-2).

30 D. Sasaqi, P. Pranoto and P. Setyono, *Caraka Tani: J. Sustain. Agric.*, 2019, **34**, 86–100.

31 B. A. Adanikin, G. A. Ogunwande and O. O. Adesanwo, Evaluation and kinetics of biogas yield from morning glory (*Ipomoea aquatica*) co-digested with water hyacinth (*Eichhornia crassipes*), *Ecol. Eng.*, 2017, **98**, 98–104, DOI: [10.1016/j.ecoleng.2016.10.067](https://doi.org/10.1016/j.ecoleng.2016.10.067).

32 G. M. Derssgeh, A. M. Melesse, S. A. Tilahun, M. Abate and D. C. Dagnew, Chapter 19 – Water hyacinth: review of its impacts on hydrology and ecosystem services—Lessons for management of Lake Tana, in *Extreme Hydrology and Climate Variability*, ed. A. M. Melesse, W. Abtew and G. Senay, Elsevier, 2019, pp. 237–251, DOI: [10.1016/B978-0-12-815998-9.00019-1](https://doi.org/10.1016/B978-0-12-815998-9.00019-1).

33 K. H. Thamaga and T. Dube, Remote sensing of invasive water hyacinth (*Eichhornia crassipes*): A review on applications and challenges, *Remote Sens. Appl.: Soc. Environ.*, 2018, **10**, 36–46, DOI: [10.1016/j.rsase.2018.02.005](https://doi.org/10.1016/j.rsase.2018.02.005).

34 A. E. Riner, J. S. Glueckert, C. J. Vuellequez, J. K. Leary, B. P. Sperry and G. E. Macdonald, Evaluation of water hyacinth (*Eichhornia crassipes*) response to herbicides using unmanned aerial system imagery, *Weed Technol.*, 2025, **39**, e59, DOI: [10.1017/wet.2025.28](https://doi.org/10.1017/wet.2025.28).

35 N. Sumrith, L. Techawinyutham, M. R. Sanjay, R. Dangtungsee and S. Siengchin, Characterization of alkaline and silane treated fibers of 'Water Hyacinth Plants' and reinforcement of 'Water Hyacinth Fibers' with bioepoxy to develop fully biobased sustainable ecofriendly composites, *J. Polym. Environ.*, 2020, **28**, 2749–2760, DOI: [10.1007/s10924-020-01810-y](https://doi.org/10.1007/s10924-020-01810-y).

36 A. Karimah, M. R. Ridho, S. S. Munawar, D. S. Adi, I. Ismadi, R. Damayanti, B. Subiyanto, W. Fatriasari and A. Fudholi, A review on natural fibers for development of eco-friendly bio-composite: characteristics, and utilizations, *J. Mater. Res.*



*Technol.*, 2021, **13**, 2442–2458, DOI: [10.1016/j.jmrt.2021.06.014](https://doi.org/10.1016/j.jmrt.2021.06.014).

37 A. Gupta, G. Singh, P. Ghosh, K. Arora and S. Sharma, Development of biodegradable tableware from novel combination of paddy straw and pine needles: A potential alternative against plastic cutlery, *J. Environ. Chem. Eng.*, 2023, **11**, 111310, DOI: [10.1016/j.jece.2023.111310](https://doi.org/10.1016/j.jece.2023.111310).

38 C. Liu, P. Luan, Q. Li, Z. Cheng, X. Sun, D. Cao and H. Zhu, Biodegradable, hygienic, and compostable tableware from hybrid sugarcane and bamboo fibers as plastic alternative, *Matter*, 2020, **3**, 2066–2079, DOI: [10.1016/j.matt.2020.10.004](https://doi.org/10.1016/j.matt.2020.10.004).

39 D. Dhanalakshmi, R. Punyamurthy and B. Basavaraju, A study of the effect of chemical treatments on areca fiber reinforced polypropylene composite properties, *Sci. Eng. Compos. Mater.*, 2017, **24**, 501–520, DOI: [10.1515/secm-2015-0292](https://doi.org/10.1515/secm-2015-0292).

40 S. Chonsakorn, S. Srivorratpaisan and R. Mongkholrattanasit, Effects of different extraction methods on some properties of water hyacinth fiber, *J. Nat. Fibers*, 2018, **16**, 1015–1025, DOI: [10.1080/15440478.2018.1448316](https://doi.org/10.1080/15440478.2018.1448316).

41 N. Muralidhar, K. Vadivuchezhian, V. Arumugam and I. S. Reddy, Flexural modulus of epoxy composite reinforced with arecanut husk fibre (AHF): A mechanics approach, *Mater. Today: Proc.*, 2020, **27**, 2265–2268, DOI: [10.1016/j.matpr.2019.09.109](https://doi.org/10.1016/j.matpr.2019.09.109).

42 M. M. Owen, E. O. Achukwu and H. Md Akil, Preparation and mechanical characterizations of water hyacinth fiber based thermoset epoxy composite, *J. Nat. Fibers*, 2022, **19**, 13970–13984, DOI: [10.1080/15440478.2022.2113850](https://doi.org/10.1080/15440478.2022.2113850).

43 S. Chaireh, P. Ngasatool and K. Kaewtatip, Novel composite foam made from starch and water hyacinth with beeswax coating for food packaging applications, *Int. J. Biol. Macromol.*, 2020, **165**, 1382–1391, DOI: [10.1016/j.ijbiomac.2020.10.007](https://doi.org/10.1016/j.ijbiomac.2020.10.007).

44 P. Senthamaraikannan and M. Kathiresan, Characterization of raw and alkali treated new natural cellulosic fiber from *Coccinia grandis* L, *Carbohydr. Polym.*, 2018, **186**, 332–343, DOI: [10.1016/j.carbpol.2018.01.072](https://doi.org/10.1016/j.carbpol.2018.01.072).

45 M. Fazaeli, Z. Emam-Djomeh, A. Kalbasi Ashtari and M. Omid, Effect of spray drying conditions and feed composition on the physical properties of black mulberry juice powder, *Food Bioprocess Technol.*, 2012, **90**, 667–675, DOI: [10.1016/j.fbp.2012.04.006](https://doi.org/10.1016/j.fbp.2012.04.006).

46 A. R. P. Kingsly, D. B. Singh, M. R. Manikantan and R. K. Jain, Moisture dependent physical properties of dried pomegranate seeds (Anardana), *J. Food Eng.*, 2006, **75**, 492–496, DOI: [10.1016/j.jfoodeng.2005.04.033](https://doi.org/10.1016/j.jfoodeng.2005.04.033).

47 H. Y. Tiong, S. K. Lim, Y. L. Lee, C. F. Ong and M. K. Yew, Environmental impact and quality assessment of using eggshell powder incorporated in lightweight foamed concrete, *Constr. Build. Mater.*, 2020, **244**, 118341, DOI: [10.1016/j.conbuildmat.2020.118341](https://doi.org/10.1016/j.conbuildmat.2020.118341).

48 R. Aidoo, I. N. Oduro, J. K. Agbenorhevi, W. O. Ellis and N. B. Pepra-Ameyaw, Physicochemical and pasting properties of flour and starch from two new cassava accessions, *Int. J. Food Prop.*, 2022, **25**, 561–569, DOI: [10.1080/10942912.2022.2052087](https://doi.org/10.1080/10942912.2022.2052087).

49 E. Elaveniya and J. Jayamuthunagai, Functional, physicochemical and anti-oxidant properties of dehydrated banana blossom powder and its incorporation in biscuits, *Int. J. ChemTech Res.*, 2014, **6**, 4446–4454.

50 B. P. Meshram, P. Jain and K. K. Gaikwad, Innovative Development of Kodo Millet (*Paspalum scrobiculatum*)-Based Functional Edible Cups Modified with Hibiscus Powder and Guar Gum: An Eco-Efficient Resource Utilization, *ACS Food Sci. Technol.*, 2025, **5**, 788–799, DOI: [10.1021/acsfoodscitech.4c00985](https://doi.org/10.1021/acsfoodscitech.4c00985).

51 S. K. H. Bukharya, F. K. Choudharya, D. N. Iqbal, Z. Ali, A. Sadiqa, S. Latif, K. M. Al-Ahmary, S. Basheer, I. Ali and M. Ahmed, Development and characterization of a biodegradable film based on guar gum-gelatin@sodium alginate for a sustainable environment, *RSC Adv.*, 2024, **14**, 19349–19361, DOI: [10.1039/D4RA03985H](https://doi.org/10.1039/D4RA03985H).

52 N. Pal and M. Agarwal, Development and characterization of eco-friendly guar gum-agar-beeswax-based active packaging film for cheese preservation, *Int. J. Biol. Macromol.*, 2024, **277**, 134333, DOI: [10.1016/j.ijbiomac.2024.134333](https://doi.org/10.1016/j.ijbiomac.2024.134333).

53 C. M. Machado, P. Benelli and I. C. Tessaro, Study of interactions between cassava starch and peanut skin on biodegradable foams, *Int. J. Biol. Macromol.*, 2020, **147**, 1343–1353, DOI: [10.1016/j.ijbiomac.2019.10.098](https://doi.org/10.1016/j.ijbiomac.2019.10.098).

54 S. Marimuthu, A. Saikumar and L. S. Badwaik, Development and characterization of biodegradable foam plates from corn starch and banana bunch stalks coated with beeswax, *Biomass Convers. Biorefin.*, 2025, **15**, 7763–7777, DOI: [10.1007/s13399-024-05782-0](https://doi.org/10.1007/s13399-024-05782-0).

55 J. S. Ng, P. L. Kiew, M. K. Lam, *et al.*, Preliminary evaluation of the properties and biodegradability of glycerol- and sorbitol-plasticized potato-based bioplastics, *Int. J. Environ. Sci. Technol.*, 2022, **19**, 1545–1554, DOI: [10.1007/s13762-021-03213-5](https://doi.org/10.1007/s13762-021-03213-5).

56 J. Tarique, S. M. Sapuan and A. Khalina, Effect of glycerol plasticizer loading on the physical, mechanical, thermal, and barrier properties of arrowroot (*Maranta arundinacea*) starch biopolymers, *Sci. Rep.*, 2021, **11**, 13900, DOI: [10.1038/s41598-021-93094-y](https://doi.org/10.1038/s41598-021-93094-y).

57 D. C. M. Ferreira, G. Molina and F. M. Pelissari, Biodegradable trays based on cassava starch blended with agroindustrial residues, *Composites, Part B*, 2020, **183**, 107682, DOI: [10.1016/j.compositesb.2019.107682](https://doi.org/10.1016/j.compositesb.2019.107682).

58 M. Y. Naz, S. A. Sulaiman, B. Ariwahjoedi and K. Z. Shaari, Characterization of modified tapioca starch solutions and their sprays for high temperature coating applications, *Sci. World J.*, 2014, **2014**, 375206, DOI: [10.1155/2014/375206](https://doi.org/10.1155/2014/375206).

59 J. Huang, M. Wei, R. Ren, H. Li, S. Liu and D. Yang, Morphological changes of blocklets during the gelatinization process of tapioca starch, *Carbohydr. Polym.*, 2017, **163**, 324–329, DOI: [10.1016/j.carbpol.2017.01.083](https://doi.org/10.1016/j.carbpol.2017.01.083).

60 A. Karnwal, G. Kumar, R. Singh, M. Selvaraj, T. Malik and A. R. M. Al Tawaha, Natural biopolymers in edible coatings: Applications in food preservation, *Food Chem.: X*, 2025, **25**, 102171, DOI: [10.1016/j.fochx.2025.102171](https://doi.org/10.1016/j.fochx.2025.102171).



61 S. Buxoo and P. Jeetah, Feasibility of producing biodegradable disposable paper cup from pineapple peels, orange peels and Mauritian hemp leaves with beeswax coating, *SN Appl. Sci.*, 2020, **2**, 1359, DOI: [10.1007/s42452-020-3164-7](https://doi.org/10.1007/s42452-020-3164-7).

62 N. J. Changmai and L. S. Badwaik, Effect of Polyvinyl Alcohol, Starch and Modified Bee Wax on Properties of Sweet Lime Pomace Based Biodegradable Containers, *J. Packag. Technol. Res.*, 2021, **5**, 107–114, DOI: [10.1007/s41783-021-00116-1](https://doi.org/10.1007/s41783-021-00116-1).

63 ISO, 536:2019, Paper and board—Determination of grammage, available online: <https://www.iso.org/standard/77583.html>, accessed 21 August 2025.

64 J. Iewkittayakorn, P. Khunthongkaew, Y. Wongnoipla, K. Kaewtatip, P. Suybangdum and A. Sopajarn, Biodegradable plates made of pineapple leaf pulp with biocoatings to improve water resistance, *J. Mater. Res. Technol.*, 2020, **9**, 5056–5066, DOI: [10.1016/j.jmrt.2020.03.023](https://doi.org/10.1016/j.jmrt.2020.03.023).

65 N. Kaisangsri, O. Kerdchoechuen and N. Laohakunjit, Biodegradable foam tray from cassava starch blended with natural fiber and chitosan, *Ind. Crops Prod.*, 2012, **37**, 542–546, DOI: [10.1016/j.indcrop.2011.07.034](https://doi.org/10.1016/j.indcrop.2011.07.034).

66 ASTM, D 644–99 (Reapproved 2002), Standard Test Method for Moisture Content of Paper and Paperboard by Oven Drying, available online: <https://file.yzimgs.com/175706/2011090910013559.pdf>, accessed 21 August 2025.

67 ISO, 535:2023, Paper and board—Determination of water absorptiveness—Cobb method, available online, <https://www.iso.org/standard/80320.html>, accessed 21 August 2025.

68 N. H. P. Rodrigues, J. T. de Souza, R. L. Rodrigues, M. H. G. Canteri, S. M. K. Tramontin and A. C. de Francisco, Starch-based foam packaging developed from a by-product of potato industrialization (*Solanum tuberosum* L.), *Appl. Sci.*, 2020, **10**, 2235, DOI: [10.3390/app10072235](https://doi.org/10.3390/app10072235).

69 M. M. Hassan, N. Tucker and M. J. Le Guen, Thermal, mechanical and viscoelastic properties of citric acid-crosslinked starch/cellulose composite foams, *Carbohydr. Polym.*, 2020, **230**, 115675, DOI: [10.1016/j.carbpol.2019.115675](https://doi.org/10.1016/j.carbpol.2019.115675).

70 ASTM, D3039/D3039M, Standard Test Method for Tensile Properties of Polymer Matrix Composite Materials, ASTM International, 2014, <https://file.yzimg.com/175706/2012061422194947.pdf>, accessed 21 August 2025.

71 J. B. Engel, A. Ambrosi and I. C. Tessaro, Development of biodegradable starch-based foams incorporated with grape stalks for food packaging, *Carbohydr. Polym.*, 2019, **225**, 115234, DOI: [10.1016/j.carbpol.2019.115234](https://doi.org/10.1016/j.carbpol.2019.115234).

72 K. Kapila, S. Kirtania, L. M. Devi, *et al.*, Potential perspectives on the use of poly (vinyl alcohol)/graphene oxide nanocomposite films and its characterization, *J. Food Meas. Char.*, 2024, **18**, 1012–1025, DOI: [10.1007/s11694-023-02264-1](https://doi.org/10.1007/s11694-023-02264-1).

73 R. Rani and L. S. Badwaik, Functional properties of oilseed cakes and defatted meals of mustard, soybean and flaxseed, *Waste Biomass Valorization*, 2021, **12**, 5639–5647, DOI: [10.1007/s12649-021-01407-z](https://doi.org/10.1007/s12649-021-01407-z).

74 N. Muralidhar, V. Kaliveeran, V. Arumugam and I. Srinivasula Reddy, A study on areca nut husk fibre extraction, composite panel preparation and mechanical characteristics of the composites, *J. Inst. Eng. (India): Ser. D*, 2019, **100**, 135–145, DOI: [10.1007/s40033-019-00186-1](https://doi.org/10.1007/s40033-019-00186-1).

75 R. S. Sahai, D. Biswas, M. D. Yadav, A. Samui and S. Kamble, Effect of alkali and silane treatment on water absorption and mechanical properties of sisal fiber reinforced polyester composites, *Metall. Mater. Eng.*, 2022, **28**, 641–656, DOI: [10.56801/MME864](https://doi.org/10.56801/MME864).

76 G. Goud and R. N. Rao, Effect of fibre content and alkali treatment on mechanical properties of Roystonea regia-reinforced epoxy partially biodegradable composites, *Bull. Mater. Sci.*, 2011, **34**, 1575–1581, DOI: [10.1007/s12034-011-0361-4](https://doi.org/10.1007/s12034-011-0361-4).

77 G. Manikandan, T. P. Sathishkumar and L. Rajeshkumar, Extraction and characterization of novel biomass-based lignocellulosic fiber *Ficus benghalensis* bark for potential green material applications, *Biomass Convers. Biorefin.*, 2025, **15**, 4835–4847, DOI: [10.1007/s13399-024-05829-2](https://doi.org/10.1007/s13399-024-05829-2).

78 L. N. Lemita, S. Deghboudj, M. Rokbi, F. M. Rekbi and R. Halimi, Characterization and analysis of novel natural cellulosic fiber extracted from *Strelitzia reginae* plant, *J. Compos. Mater.*, 2022, **56**, 99–114, DOI: [10.1177/00219983211049285](https://doi.org/10.1177/00219983211049285).

79 C. M. Machado, P. Benelli and I. C. Tessaro, Sesame cake incorporation on cassava starch foams for packaging use, *Ind. Crops Prod.*, 2017, **102**, 115–121, DOI: [10.1016/j.indcrop.2017.03.007](https://doi.org/10.1016/j.indcrop.2017.03.007).

80 L. R. P. F. Mello and S. Mali, Use of malt bagasse to produce biodegradable baked foams made from cassava starch, *Ind. Crops Prod.*, 2014, **55**, 187–193, DOI: [10.1016/j.indcrop.2014.02.015](https://doi.org/10.1016/j.indcrop.2014.02.015).

81 D. Behera, S. S. Pattnaik, S. S. Patra, A. K. Barick, J. Pradhan and A. K. Behera, Development and characterization of water hyacinth reinforced thermoplastic starch as sustainable biocomposites, *RSC Sustain.*, 2025, **3**, 1807–1818, DOI: [10.1039/D4SU00803K](https://doi.org/10.1039/D4SU00803K).

82 C. M. Machado, P. Benelli and I. C. Tessaro, Constrained Mixture Design to Optimize Formulation and Performance of Foams Based on Cassava Starch and Peanut Skin, *J. Polym. Environ.*, 2019, **27**, 2224–2238, DOI: [10.1007/s10924-019-01518-8](https://doi.org/10.1007/s10924-019-01518-8).

83 J. Yang, Y. Li, X. Li, M. Ji, S. Peng, J. Man, L. Zhou, F. Li and C. Zhang, Starch-fiber foaming biodegradable composites with polylactic acid hydrophobic surface, *Int. J. Biol. Macromol.*, 2024, **267**, 131406, DOI: [10.1016/j.ijbiomac.2024.131406](https://doi.org/10.1016/j.ijbiomac.2024.131406).

84 F. J. Aranda-García, R. González-Núñez, C. F. Jasso-Gastinel and E. Mendizabal, Water absorption and thermomechanical characterization of extruded starch/poly (lactic acid)/agave bagasse fiber bioplastic composites, *Int. J. Polym. Sci.*, 2015, **2015**, 343294, DOI: [10.1155/2015/343294](https://doi.org/10.1155/2015/343294).

85 M. P. Harikrishnan, A. Thampi, A. M. Nandhu Lal, A. S. Warrier, M. Basil and A. Kothakota, Effect of



chitosan-based bio coating on mechanical, structural and physical characteristics of microfiber based paper packaging: An alternative to wood pulp/plastic packaging, *Int. J. Biol. Macromol.*, 2023, **253**, 126888, DOI: [10.1016/j.ijbiomac.2023.126888](https://doi.org/10.1016/j.ijbiomac.2023.126888).

86 P. R. Salgado, V. C. Schmidt, S. E. Molina Ortiz, A. N. Mauri and J. B. Laurindo, Biodegradable foams based on cassava starch, sunflower proteins and cellulose fibers obtained by a baking process, *J. Food Eng.*, 2008, **85**, 435–443, DOI: [10.1016/j.jfoodeng.2007.08.005](https://doi.org/10.1016/j.jfoodeng.2007.08.005).

87 A. I. Quilez-Molina, J. F. Le Meins, B. Charrier and M. Dumon, Starch-fibers composites, a study of all-polysaccharide foams from microwave foaming to biodegradation, *Carbohydr. Polym.*, 2024, **328**, 121743, DOI: [10.1016/j.carbpol.2023.121743](https://doi.org/10.1016/j.carbpol.2023.121743).

88 P. Cerruti, G. Santagata, G. Gomez d'Ayala, V. Ambrogi, C. Carfagna, M. Malinconico and P. Persico, Effect of a natural polyphenolic extract on the properties of a biodegradable starch-based polymer, *Polym. Degrad. Stab.*, 2011, **96**, 839–846, DOI: [10.1016/j.polymdegradstab.2011.02.003](https://doi.org/10.1016/j.polymdegradstab.2011.02.003).

89 P. Cinelli, E. Chiellini, J. W. Lawton and S. H. Imam, Foamed articles based on potato starch, corn fibers and poly(vinyl alcohol), *Polym. Degrad. Stab.*, 2006, **91**, 1147–1155, DOI: [10.1016/j.polymdegradstab.2005.07.001](https://doi.org/10.1016/j.polymdegradstab.2005.07.001).

90 C. M. Jaramillo, T. J. Gutiérrez, S. Goyanes, C. Bernal and L. Famá, Biodegradability and plasticizing effect of yerba mate extract on cassava starch edible films, *Carbohydr. Polym.*, 2016, **151**, 150–159, DOI: [10.1016/j.carbpol.2016.05.025](https://doi.org/10.1016/j.carbpol.2016.05.025).

91 W. Sanhawong, P. Banhalee, S. Boonsang and S. Kaewpirom, Effect of concentrated natural rubber latex on the properties and degradation behavior of cotton-fiber-reinforced cassava starch biofoam, *Ind. Crops Prod.*, 2017, **108**, 756–766, DOI: [10.1016/j.indcrop.2017.07.046](https://doi.org/10.1016/j.indcrop.2017.07.046).

92 S. Nida, J. A. Moses and C. Anandharamakrishnan, 3D printed food package casings from sugarcane bagasse: a waste valorization study, *Biomass Convers. Biorefin.*, 2025, **15**, 1835–1845, DOI: [10.1007/s13399-021-01982-0](https://doi.org/10.1007/s13399-021-01982-0).

